April 2013

Twisted Light Experimental

Sabbir M. Rashid
Worcester Polytechnic Institute

Twisted Light Experimental

Project Number: MQP-RSQ-1202

A Major Qualifying Project Report:

Submitted to the Faculty

of the

WORCESTER POLYTECHNIC INSTITUTE

In partial fulfillment of the requirements for the

Degree of Bachelor of Science

By:

Sabbir Rashid

April 25^{th}, 2013

Approved:

Prof. Richard S. Quimby, Major Advisor

Abstract

The goal of this project is to first present a detailed explanation and analysis of light with Orbital Angular Momentum (OAM), and then determine the optimal waveguide profile for the transfer of light with OAM through an optical fiber. In particular, the ring index variation fiber was studied. The explanation describes different laser modes and what it means for light to have OAM. This was accomplished by exploring the available literature on the topic. The analysis involves solving Maxwell's equations for a three-layer fiber in order to determine a characteristic equation, the solution of which can be used to make modal charts. The general results can then be used to solve for variations of waveguide designs, with the task of creating laser mode profile plots in mind. The mode plots, which are useful in determining the degeneracy of waveguide modes, are then to be evaluated to determine which type of waveguide will be best for the transferring of light with OAM.

Acknowledgements

I would like to begin this report by thanking those who helped throughout this project. I owe a debt of gratitude to Professor Richard S. Quimby, for his invaluable advice and commitment to providing the resources needed to make this MQP possible, as well as his unwavering support during this project. Furthermore, I would like to thank Caleb A. Ruvich, who worked on the experimental aspect in a related project, providing a constant reminder of the applications that can arrive from the theory. Finally, I would like to thank all the numerous students who spent long hours in the Physics lounge, busy with their own work, yet quick to provide help when needed.

Contents

1 INTRODUCTION

"Probably only physicists know that circularly polarized light carries with it an angular momentum that results from the spin of individual photons. Few physicists realize, however, that a light beam can also carry orbital angular momentum associated not with photon spin but with helical wavefronts...In many instances orbital angular momentum behaves in a similar way to spin. But this is not always so: orbital angular momentum has its own distinctive properties and its own distinctive optical components." Miles Padgett & Les Allen (Padgett and Allen, 2000)

1.1 What does it mean for Light to have Orbital Angular Momentum?

By the definition of angular momentum, which mathematically is the cross product of linear momentum and a position vector, it is apparent that any propagating light beam must have an external angular momentum associated with it, merely by choosing a nonzero position vector, or in other words, letting the point of interest be at a point removed from the axis of propagation. Furthermore it has been known for some time that photons, or individual particles of light, possess Spin Angular Momentum due to the circular polarization of the light. To understand why this is true, consider the Poynting vector, which represents the rate of energy transfer per unit area of an Electromagnetic field, defined mathematically as the cross product of the Electric and Magnetic Fields. Spin Angular Momentum is defined (generally, in the paraxial limit) by the integral of a similar cross product, between the Electric Field and the Magnetic Vector Potential. A beam of light with a circularly polarized planar wavefront has a finite cross product with the Electric Field. Therefore, integrating the cross section of the beam of light results in a finite value, which represents that there is a spin component of the light (Padgett and Allen, 2000). This form of angular momentum exists independent of the choice of coordinates, and is thus considered an internal angular momentum. More recently, however, research in the 1990s showed that for certain types of light there is another form of internal angular momentum, associated with the wavefront of the propagating light, known as Orbital Angular Momentum.

The study of Orbital Angular Momentum (OAM) Light arose from the field known as Singular Optics, which arose in the 1970s theoretically centered on optical vortices. An optical vortex is a point of zero intensity, or a singularity, in an optical field produced by destructive interference. This singularity arises when light is twisted around its axis of travel, like a corkscrew, causing the axial light waves to cancel each other out. When projected on a flat screen, the wavefront appears as a ring with a dark

spot at its center. By twisting around its axis, the light beam creates a helical wavefront, which has orbital angular momentum, as made apparent by Miles Padgett and Les Allen in the opening quote of this section.

1.2 Are there any Practical Applications of OAM light?

The most promising applications of light with orbital angular momentum involve the field of quantum communication, where optical messages are classically sent in the form of photons that can have two spin states. These two spin states correspond to the two types of circular polarizations available for a light beam, either a clockwise or counterclockwise rotation of the electric field. Normally, each of these spin states are used to represent one binary digit, or bit, while the other state represents the remaining binary digit (Minkel). For example, a clockwise rotation may represent the bit 1 while a counterclockwise rotation may represent the bit 0. In this manner, the optical information may be encoded one bit at a time. However, by using orbital angular momentum measurements, which may take on an infinite number of values, the amount of information that may be encoding at a time will greatly increase. In an article written by Jonathan Leach and M. J. Padgett from the University of Glasgow, as well as three colleagues from the University of Strathclyde, an interferometric method, or process involving the use of interference patterns, for measuring the orbital angular momentum of single photons is proposed, making the use of orbital angular momentum states as an alphabet for optical communications feasible possibility, since implications of this approach include entanglement experiments, quantum cryptography and high density information transfer (Leach, Padgett and Barnett, 2002).

The possible uses of the orbital angular momentum in optical communications is further increased by the work of Marrucci, Manzo and Papro, who experimentally demonstrate an optical process in which the spin angular momentum is converted into orbital angular momentum, allowing for input polarization to be used to generate helical modes with a wave-front helicity (Marrucci, Manzo and Papro, 2006). Their method takes advantage of the conversion of angular momentum. Since the amount of information that can be carried in an orbital momentum state is greater than that for spin states, the ability to manipulate the orbital components of a light beam could lead to new communication methods. Furthermore, new kinds of logic operations in future optical computers may be made possible by controlling the interaction of spin and orbital angular momentum in the same photon (Lindley, 2006).

1.3 What are some problems with Light with OAM?

While there are numerous promising possibilities involving the encoding of information in OAM light, the actual propagation of this light has proven to be a challenge. In processes involving propagation the structure of the light beam may change, since light beams with OAM are susceptible to atmospheric scintillation, where light is absorbed and reemitted usually with less energy (Bozinovic, Kristensen and Ramachandran, Long-range fiber transmission, 2011). Furthermore, to retain light with OAM specific linear combinations of waveguide modes are required. For example, a combination two HE_{21} modes with a phase shift difference of $\pm\pi/2$ will result in OAM states, but the slightest perturbation may cause these modes to couple with TE_{01} or TM_{01} modes, resulting in the creation of undesired Hermite-Gaussian beams (Ramachandran, Kristensen and Yan, 2009). Hermite-Gaussian modes arise when solving the paraxial Helmholtz equation in Cartesian coordinates, and typically do not result in the radial symmetry required for light with OAM. (On the other hand, Laguerre-Gaussian modes arise when solving the paraxial Helmholtz equation in Polar coordinates, and result in the radial symmetry required for light with OAM.) Therefore, due the problems mentioned above, light with OAM is conventionally considered to be unstable in optical fibers. In order for OAM light to progress through a fiber, the TE_{01}, TM_{01}, and the HE_{21} modes cannot couple. Thus, for OAM light propagation, an optical fiber must be designed such that degeneracy in these three modes do not occur for long distances. To understand the physical meaning of coupling of modes, consider the following figure, where the lines connecting the three aforementioned modes are used to depict the result of coupling between these modes.

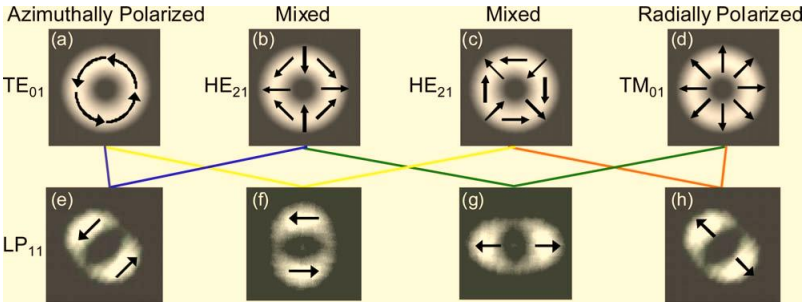

Figure 1: Ramachandran, et al. Undesired Modal Coupling

As shown above, different combinations of TE_{01}(a), TM_{01}(b), and the HE_{21}(c,d) modes result in different orientations of undesired linearly polarized LP_{11}(e,f,g,h) modes.

1.4 What progress have people made in this field?

By the final decade of the twentieth century, when optical fields with wavefront dislocations were being produced experimentally, the production of optical vortex dislocations of different orders was first described in the Journal of Experimental and Theoretical Physics, in a 1990 paper by V. Yu. Bazhenov, M. V. Vasnetsov, and M.S. Soskin. As shown below in Figure 2, the experimental apparatus used by Bazhenov and his colleagues consisted of a He-Ne Laser (1), beam expander (2), beam splitter (3), mirrors (4,5), objective lens (6), braided optical fibers (7), diverging lens (8), half-silvered mirror (9), camera (10), and a screen for observing the interference of the beam (11). With this setup they were able to demonstrate the existence of orbital angular momentum and a helical wave surface, through the observation of a singularity at the wave center (Bazhenov, Vasnetsov and Soskin, 1990).

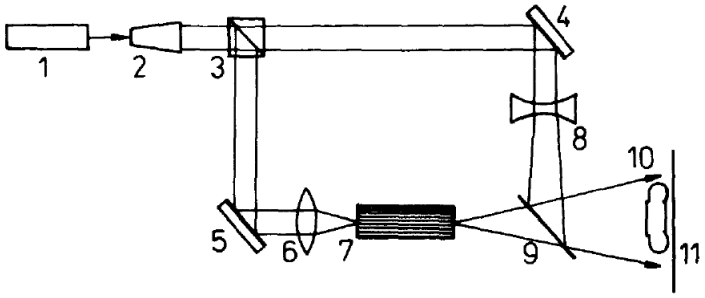

Figure 2: Bazhenov, et al. Experimental Setup

The next landmark paper was published in 1992 in the Physical Review A, written by Les Allen, M. W. Beijersbergen, R. J. C. Spreeuw, and J. P. Woerdman. In this paper, Allen and his colleagues demonstrated that a well-defined orbital angular momentum equal to $l\hbar$ per photon could be found from a Laguerre-Gaussian laser mode, where $\hbar$ is the reduced Planck constant, and l is the azimuthal mode index (Allen, Beijersbergen and Spreeuw, 1992). They also outlined how it was possible to convert the orbital angular momentum into mechanical torque by using astigmatic optical elements, which may also be used to produce Laguerre-Gaussian modes from Hermite-Gaussian modes (Allen, Beijersbergen and Spreeuw, 1992). In other words, they discovered a method of converting light beams that don't have OAM into those that do. Furthermore, Allen, et al. determined that all non-planar light beams (which possess field gradients) have to some degree a measure of orbital angular momentum.

Since then, numerous papers have been written involving light with OAM, its detection, and creation, including the work of Ranjeet Kumar, M. Harris, Yang Yue and their colleagues. With the ability to create light with OAM confirmed, and the theory behind it well established, the major problem remaining

was the propagation of light with OAM. Attempts to solve this problem began around the same time that the 1992 L. Allen paper described above came out, when I. V Neves and A. S. C. Fernandes wrote a paper presenting analytical solutions for the propagation of waves in a general inhomogeneous dielectric medium in a cylindrical coordinate system (Neves and Fernandes, 1992). This was done by solving Maxwells Equations to determine the Electric and Magnetic Field components, which were expanded into a series solution of the Frobenius Type, which includes Bessel functions in a homogeneous medium, and the Taylor Type, which was new at the time and allowed for the construction of a general and fast convergent algorithm for computing the modal characteristics of the waves (Neves and Fernandes, 1992). Using this method, Neves and Fernandes were able to make the dielectric profile plot shown in Figure 3 below.

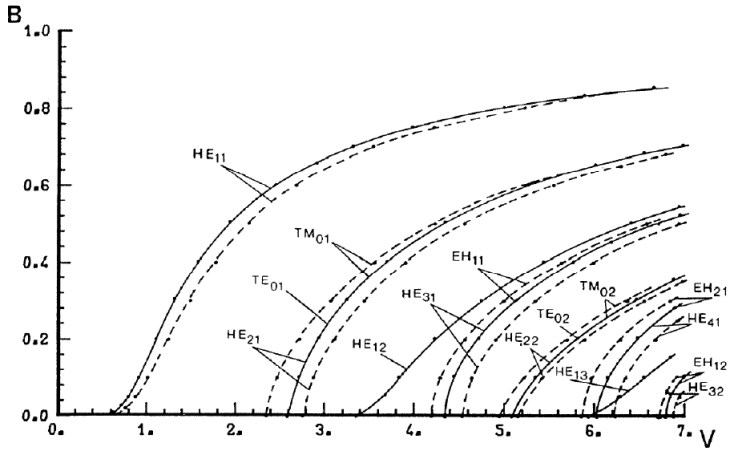

Figure 3: Neves and Fernandez Gaussian dielectric profile

The significance of such plots is that they allow for a graphical visualization of the modes in an optical fiber, allowing the degeneracy, or overlapping, of certain modes to be clearly viewed. As degeneracy causes modal coupling, which is undesired for certain combinations of modes, by observing the profile plot of a waveguide can reveal whether a certain type of light will or will not propagate through it without distortion. As mentioned in the previous section, in order for OAM light to progress through a fiber, the TE_{01}, TM_01 , and the HE_21 modes cannot couple. This coupling, or degeneracy, occurs when the modal curves above overlap.

By 1997, Neves and Fernandes were able to construct A-type profile plots, which concerned optical fibers with the greatest dielectric value at the center of the core, or origin, which would decrease as you moved radially outward, to settle at a minimum value at the cladding region; and V- type profile

plots, which began at a minimum value, would increase as you moved radially outward, but again have a minimum value at the cladding region. Examples of the dielectric structure of these profile plots are shown below in Figure 4.

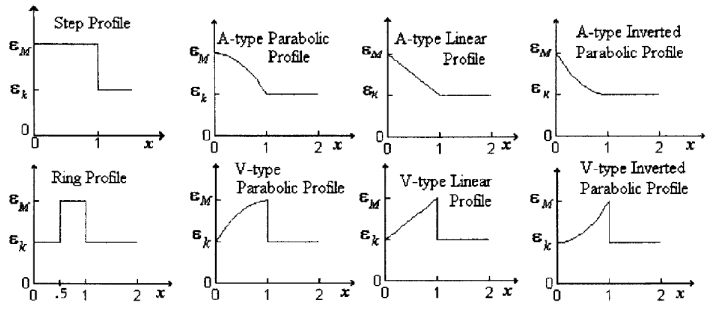

Figure 4: Neves and Fernandez A and V-type dielectric profiles

By the end of the twentieth century, Neves and Fernandes were able to construct W-type profile plots, which concerned optical fibers with the greatest dielectric value at the origin, which would decrease to a minimum as you moved radially outward, and finally settle at an intermediate value at the cladding region; and V- type profile plots, which began at a minimum value, would increase as you moved radially outward to a maximum value, but finally settle at an intermediate value at the cladding region. Examples of the dielectric structure of these profile plots are shown below in Figure 5.

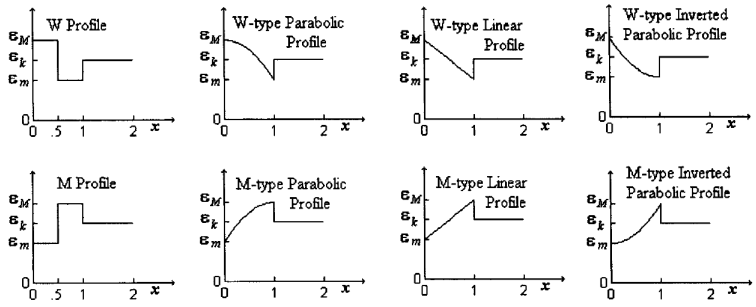

Figure 5: Neves and Fernandez W and M-type dielectric profiles

Relatively recently, in 2009 Siddharth Ramachandran, Poul Kristensen and Man F. Yan, looking to address the problem of OAM light propagation, designed a fiber with a purity, defined as the ratio of the specific optical rotation of a sample to the specific optical rotation of the pure rotating light wave, of over 99.8% which removed the near degeneracy of the TE_{01}, TM_{01} modes and HE_{21} modes, allowing light with OAM to propagate to a length slightly over 20 meters (Ramachandran, Kristensen and Yan, 2009). Merely two years later, working with Nenad Bozinovic, Ramachandran's team was able to achieve

a propagation length of 0.9 km, which a purity of 97% (Bozinovic, Kristensen and Ramachandran, Are OAM/Vortex States of Light, 2011). The length of 0.9 km corresponds to the amount of fiber the team had available, and 2 of the 3 percent of degradation in purity occurred within the first 100 meters, so greatly lengths of propagation is very probable. Furthermore, less than 20 decibels of cross-talk, or undesired coupling effects, was measured at the output (Bozinovic, Kristensen and Ramachandran, Long-range fiber transmission, 2011). With such advances, the use of OAM light in quantum communication applications becomes a real possibility.

2 THEORY

In the 1999 article by L. Allen, M. J. Padgett and M. Babiker, the mathematical analysis of what it means for light to have OAM was derived. Therefore, the complete argument is not repeated here, but rather an overview of the results is presented. The argument presented by Allen and his colleagues begins with the paraxial approximation, which assumes that the light beam is reasonably well collimated and does not diverge too much as it propagates in the positive z-direction. This approximation results in the paraxial wave equation

$$j\frac{\partial u}{\partial z} = -\frac{1}{2k}\left(\frac{\partial^2}{\partial x^2} + \frac{\partial^2}{\partial y^2}\right)u \quad , \tag{1}$$

where $u(x, y, z)$ is the amplitude distribution of the wave and j is the square root of -1. Using the Lorenz gauge condition ($\partial_\mu A^\mu = 0$) to fix the magnetic vector potential, which was taken to be polarized along the x-direction ($\mathbf{A} = \hat{x}ue^{jkz}$), results in the magnetic and electric fields

$$\mathbf{B} = \mu_0\mathbf{H} = jk\left[u\hat{y} + \frac{j}{k}\frac{\partial u}{\partial y}\hat{z}\right]e^{jkz} \quad , \tag{2}$$

$$\mathbf{E} = jk\left[u\hat{x} + \frac{j}{k}\frac{\partial u}{\partial y}\hat{z}\right]e^{jkz} \quad . \tag{3}$$

These values are used to find the time averaged Poynting Vector

$$\mathbf{S} = \epsilon_0\langle\mathbf{E}\times\mathbf{B}\rangle = j\omega\frac{\epsilon_0}{2}(u\nabla u^* - u^*\nabla u) + \omega k\epsilon_0 \mid u \mid^2 \hat{z} \quad . \tag{4}$$

From this result, and writing u in polar coordinates $u(\rho, \phi, z) = u_0(\rho, z)e^{jl\phi}$, the angular momentum density j is found to be

$$j_z = \epsilon_0\omega l \mid u \mid^2 \quad , \tag{5}$$

and the energy density w is found to be

$$w = \epsilon_0\omega^2 \mid u \mid^2 \quad . \tag{6}$$

Integrating these two quantities results in the total angular momentum J and total energy W. Taking the ratio of the angular momentum and energy results in

$$\frac{j_z}{w} = \frac{J_z}{W} = \frac{l}{\omega} = \frac{l\hbar}{\omega\hbar} \quad . \tag{7}$$

The significance of this result is that it hints at a well-defined orbital angular momentum equal to $l\hbar$ per photon. However, this result was found in the paraxial approximation, and by taking a magnetic vector potential that was polarized only along the x-direction. To further generalize the result, while remaining within the realm of the paraxial approximation, consider a circularly polarized magnetic vector potential $\mathbf{A} = (\alpha\hat{x} + \beta\hat{y})ue^{jkz}$. In this case, the resulting time averaged Poynting Vector

$$\mathbf{S} = \epsilon_0\langle \mathbf{E} \times \mathbf{B} \rangle = \frac{\epsilon_0}{2}\left[j\omega(u\nabla u^* - u^*\nabla u) + 2\omega k\epsilon_0 \mid u \mid^2 \hat{z} + j\omega(\alpha\beta^* - \alpha^*\beta)\left(\frac{\partial}{\partial y}\hat{x} - \frac{\partial}{\partial x}\hat{y}\right) \mid u \mid^2 \right] \quad . \tag{8}$$

Using this result, and denoting the helicity, or component of intrinsic angular momentum along the direction of propagation, as σ, the ratio of the total angular momentum and total energy results in

$$\frac{J_z}{W} = \frac{l+\sigma}{\omega} = \frac{l\hbar}{\omega\hbar} + \frac{\sigma\hbar}{\omega\hbar} \quad . \tag{9}$$

This result reveals that a circularly polarized beam has a spin angular momentum, equal to $\sigma\hbar$ per photon, as well as the orbital angular momentum equal to $l\hbar$ per photon. Furthermore, the result implies that these two terms are separable, that the angular momentum is comprised of a spin term and an orbital term, since they are linearly independent and the spin term appeared only after the introduction of circular polarization. However, this result is only valid when taking the paraxial approximation. When the analysis is attempted outside the realm of the paraxial approximation, the resulting ratio of the total angular momentum and total energy is

$$\frac{J_z}{W} = \frac{l+\sigma}{\omega} + \frac{\sigma}{\omega}\left[\frac{\int_0^k d\kappa \frac{|E(\kappa)|^2\kappa}{(k^2-\kappa^2)}}{\int_0^k d\kappa \frac{|E(\kappa)|^2(2k^2-\kappa^2)}{\kappa(k^2-\kappa^2)}} \right] \quad . \tag{10}$$

This result reveals an additional correction term for the paraxial approximation. Furthermore, due to this term, the orbital and spin terms cannot be simply separated. Therefore, it would not be correct in considering the total angular momentum as a sum of a spin term and an orbital term.

3 METHODOLOGY

The main goal of this project was to create modal profile plots to determine the optimal design of an optical fiber for the transmission of OAM light. More specifically, ring fiber profile plots were explored. In this section, the methods used in the execution of this goal are described. As this project was a theoretical one, experimental materials were not required. However, the use of a computer was necessary, as well as computing software. In this regard, the most important tool that aided in the completion of the research was MATLAB.

The first step taken toward progressing towards the goal was the conduction of research and becoming familiar with light with Orbital Angular Momentum. While there are a lot of research papers written on the subject of OAM light, these articles can be separated into various categories. For example, the work done by Les Allen and his colleagues provide both an introduction to the topic as well as a mathematical analysis. On the other hand, work done by Ramachandran and his colleagues focus more on the generation of OAM light and its propagation. Furthermore, research was conducted to further the understanding of propagation of light through optical fibers. For example, the work done by Neves and Fernandes did not focus specifically on OAM light, but rather on modal characteristics and the effects of different dielectric materials in the construction of optical fibers. The combination of the different types of articles aided in gaining a copious perception of both OAM light and propagation of light through optical fibers.

After gaining an ample understanding of OAM light, it was necessary to then understand the process of making modal profile plots. This was done by using Maxwell's equations to derive the characteristic equations for a step-index fiber, and then solving the characteristic equations to create mode plots. The analysis conducted used the Boundary Value Problem approach, and is provided in Appendix A. The resulting plots of the variables in the characteristic equations, Ka and γa, closely agreed with the results found in Iizuka's related argument in his fiber optics textbook. This confirmed that the analysis conducted was correct. However, at this point the understanding of modal charts was not complete, and it was not realized that the Ka vs. γa were not mode plots. Rather, the intersection of these curves and a normalized radius, V, determined the points that comprised a mode chart.

This approach provided preparation for the next step of the project, which was an attempt at ana-

lytically solving the Boundary Value Problem for a three layer fiber, which is provided in Appendix B. A quick glance at Appendices A and B will reveal that while the same approach used in solving the 2-layer problem was used for the 3-layer problem, this method resulted in too many unknown coefficients to easily analytically solve for.

Therefore, a computational series approach was decided to be a better approach to take. One such paper that used a series method was written by Neves and Fernandes, which was published in 1992. This paper suggested using Frobenius Series type solutions for the outer and inner fiber layer, while using Taylor Series to solve for the intermediate layer. Subsequent papers by these authors used this method to create modal profile plots for various dielectric fiber structures. A significant portion of the project was spent exploring the work of Neves and Fernandes, with the belief that it would allow for the quick construction of profile plots. However, due to the ommitance of fundamental steps and details in their papers, the replication of the results proved to be impervious. Thus, it was necessary to find another way to create the profile plots.

The inspiration for a new method of solving the 3-layer waveguide problem came from an electrical engineering article, rather than one in optics, by Hongchin Lin and Kawthar A. Zaki. In the paper they present the general solution to a 3-layer dielectric loaded waveguide. The main difference between a loaded waveguide and an optical fiber is related to the outer most layer. In an optical fiber the outer most layer is designed such that the light beam travelling through the fiber does not escape. On the other hand, for a loaded waveguide the outer most layer is connected to a perfectly conducting wall, which would allow for the electromagnetic wave to escape. Nevertheless, in the limit that the third layer becomes infinitely large an electromagnetic wave would not be able to escape either fiber, and thus the two situations become theoretically identical. Therefore, in order to achieve the goal of this project the solution to Maxwell's equations found in the Lin paper and the resulting characteristic equations in the limit that the third layer becomes infinitely large were used.

4 RESULTS

In the paper mentioned in the previous section, Lin and Zaki find the characteristic equation of the 3-layer waveguide to be of the form

$$T_n U_n - k_0^2 a^2 V_n W_n = 0 \quad , \tag{11}$$

where k_0 is the free space wave number, a is the radius of the core layer, and

$$T_\nu = (-M_2 S_{a'b} + M_1 S_{ab'} - M_1 \frac{\tau_2 a}{\tau_3 a} \frac{R_{b'c'}}{R_{bc'}} S_{ab}) J_\nu(\xi_1 a) - M_2 \frac{\tau_2 a}{\xi_1 a} \frac{\epsilon_{r1}}{\epsilon_{r2}} S_{ab} J'_\nu(\xi_1 a) \quad , \tag{12}$$

$$U_\nu = (M_2 S_{a'b} - M_1 S_{ab'} + M_1 \frac{\tau_2 a}{\tau_3 a} \frac{R_{b'c}}{R_{bc}} S_{ab}) J_\nu(\xi_1 a) + M_2 \frac{\tau_2 a}{\xi_1 a} S_{ab} J'_\nu(\xi_1 a) \quad , \tag{13}$$

$$V_\nu = (-M_1 M_2 \frac{\tau_2 a}{(k_0 a)^2 \epsilon_{r2}} S_{ab} + \frac{S_{a'b'}}{\tau_2 a} - \frac{R_{b'c'}}{R_{bc'}} \frac{S_{a'b}}{\tau_3 a}) J_\nu(\xi_1 a) + (S_{ab'} - \frac{\tau_2 a}{\tau_3 a} \frac{R_{b'c'}}{R_{bc'}} S_{ab}) \frac{J'_\nu(\xi_1 a)}{\xi_1 a} \quad \text{and} \tag{14}$$

$$W_\nu = (-M_1 M_2 \frac{\tau_2 a}{(k_0 a)^2} S_{ab} + \frac{\epsilon_{r2} S_{a'b'}}{\tau_2 a} - \frac{R_{b'c'}}{R_{bc}} \frac{\epsilon_{r2}}{\tau_3 a} S_{a'b}) J_\nu(\xi_1 a) + (S_{ab'} - \frac{\epsilon_{r3}}{\epsilon_{r2}} \frac{\tau_2 a}{\tau_3 a} \frac{R_{b'c}}{R_{bc}} S_{ab}) \frac{\epsilon_{r1} J'_\nu(\xi_1 a)}{\xi_1 a} \tag{15}$$

are functions of what are referred to as the cutoff wave numbers of the medium: $\xi_1 = \sqrt{k_1^2 - \beta^2}$ in the core layer, $\tau_2 = \sqrt{\beta^2 - k_2^2}$ in the intermediate layer, $\tau_3 = \sqrt{\beta^2 - k_2^2}$ in the cladding layer, with $k_i = \sqrt{k_0^2 \epsilon_{ri}}$. In the above equations J_ν and J'_ν are the Bessel function of the first kind and its derivative, respectively. Incorporated into the equations are the terms

$$M_1 = \beta a \nu \left[\frac{1}{(\xi_1 a)^2} + \frac{1}{(\tau_2 a)^2} \right] \quad , \tag{16}$$

$$M_2 = \frac{\beta a \nu}{b/a} \left[\frac{1}{(\tau_3 a)^2} - \frac{1}{(\tau_2 a)^2} \right] \quad , \tag{17}$$

$$S_{ab} = I_\nu(\tau_2 a) K_\nu(\tau_2 b) - K_\nu(\tau_2 a) I_\nu(\tau_2 b) \quad , \tag{18}$$

$$S_{a'b} = I'_\nu(\tau_2 a) K_\nu(\tau_2 b) - K'_\nu(\tau_2 a) I_\nu(\tau_2 b) \quad , \tag{19}$$

$$S_{ab'} = I_\nu(\tau_2 a) K'_\nu(\tau_2 b) - K_\nu(\tau_2 a) I'_\nu(\tau_2 b) \quad , \tag{20}$$

$$S_{a'b'} = I'_\nu(\tau_2 a) K'_\nu(\tau_2 b) - K'_\nu(\tau_2 a) I'_\nu(\tau_2 b) \quad , \tag{21}$$

$$R_{bc} = I_\nu(\tau_3 b) K_\nu(\tau_3 c) - K_\nu(\tau_3 b) I_\nu(\tau_3 c) \quad , \tag{22}$$

$$R_{b'c} = I'_\nu(\tau_3 b) K_\nu(\tau_3 c) - K'_\nu(\tau_3 b) I_\nu(\tau_3 c) \quad , \tag{23}$$

$$R_{bc'} = I_\nu(\tau_3 b)K'_\nu(\tau_3 c) - K_\nu(\tau_3 b)I'_\nu(\tau_3 c) \quad , \tag{24}$$

$$R_{b'c'} = I'_\nu(\tau_3 b)K'_\nu(\tau_3 c) - K'_\nu(\tau_3 b)I'_\nu(\tau_3 c) \quad , \tag{25}$$

where b is the radius of the intermediate layer, c is the radius of the cladding layer, and I_ν & K_ν are the modified Bessel functions of the first and second kinds, respectively, of order ν and the prime notation is used to represent their derivatives. As mentioned in the previous section, the results of the Lin paper for a 3-layer loaded waveguide can correspond to that for an optical fiber by extending c to infinity. However, consider the following argument. An immediate property of the modified Bessel function of the first kind and its derivatives is that they approach infinity as its arguments approach infinity. An immediate property of the modified Bessel function of the second kind and its derivatives is that they approach zero as its arguments approach infinity. Furthermore, the modified Bessel function of the first kind has the recursion relation $I_\nu = I_{\nu-1}$ while the second kind has the recursion relation $K_\nu = -K_{\nu-1}$. Therefore, it follows that as c goes to infinity,

$$R_{bc} \to -\infty \tag{26}$$

$$R_{b'c} \to \infty \tag{27}$$

$$R_{bc'} \to -\infty \tag{28}$$

$$R_{b'c'} \to \infty \quad . \tag{29}$$

In the characteristic equation, the above terms that approach infinity are always paired in a quotient with a term that approaches negative infinity, and vice-versa. Therefore, in order to continue the analysis, the simplification was taken such that these pairs were set equal to -1. However, this approach is not mathematically permissible without proof, and in this case does lead to unexpected results which will be discussed later in the following section. An alternate approach to dealing with these non-well-behaved functions is discussed in the Future Work section.

A special case of the characteristic equation above occurs when $\nu = 0$. This results in what are known as meridional modes, which are either Transverse Electric (TE) or Transverse Magnetic (TM). In these cases the terms T_ν and U_ν become 0. Therefore, in order for the characteristic equation to be satisfied, either $V_\nu = V_0$ or $W_\nu = W_0$ have to equal 0. The case where $V_0 = 0$ corresponds to TE modes, which

can be solved for in terms of the cutoff wave numbers. In this case,

$$V_0 = (\frac{S_{a'b'}}{\tau_2 a} - \frac{R_{b'c'}}{R_{bc'}}\frac{S_{a'b}}{\tau_3 a})J_0(\xi_1 a) + (S_{ab'} - \frac{\tau_2 a}{\tau_3 a}\frac{R_{b'c'}}{R_{bc'}}S_{ab})\frac{J_0'(\xi_1 a)}{\xi_1 a} \quad . \tag{30}$$

This equation was then simplified using recursion relations and the quotient approximation mentioned above, and then used to determine relationships for the cutoff wave numbers. The resulting curve for the cutoff wave number of the core ξ_1 when plotted vs. τ_3 is shown below in figure 6.

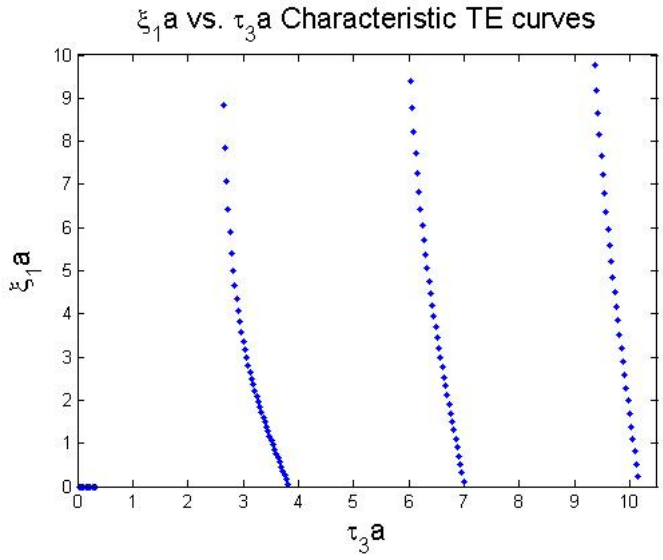

Figure 6: TE Characteristic Equation plot for ξ_1

In this case a normalized radius (not to be confused with V_ν or V_0) defined as $V = \sqrt{\xi_1^2 + \tau_3^2}$ corresponds to the radius of a circle centered at the origin of the above plot. For a step-index fiber, the intersection of the circle with the TE Characteristic equation curve would correspond to modal points. An analogous modal plot is shown below, with the normalized radius written in terms of the dielectric permittivity of the layers.

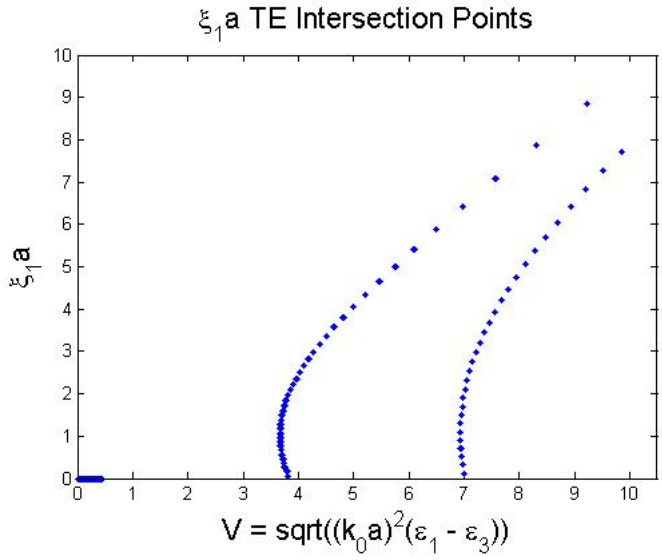

Figure 7: ξ_1 TE Intersection Points with V parameter

Similarly, the TE Characteristic Equation can be used to solve for in terms of τ_2. The resulting plot is shown below.

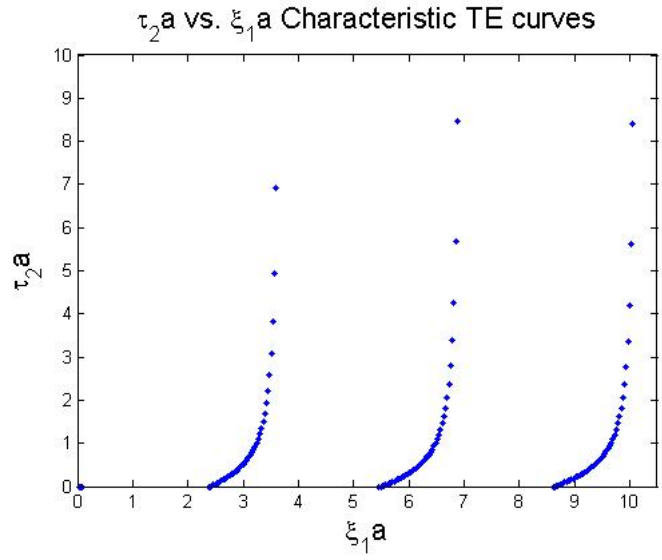

Figure 8: TE Characteristic Equation plot for τ_2

In this case, in order for the Normalized Radius to correspond to the radius of a circle centered at the origin, it must be defined as $V = \sqrt{\xi_1^2 + \tau_2^2}$. The resulting modal chart is plotted below. In terms of the dielectric permittivity of the layers, $V = \sqrt{(k_0 * a)^2(\epsilon_1 - \epsilon_2)}$.

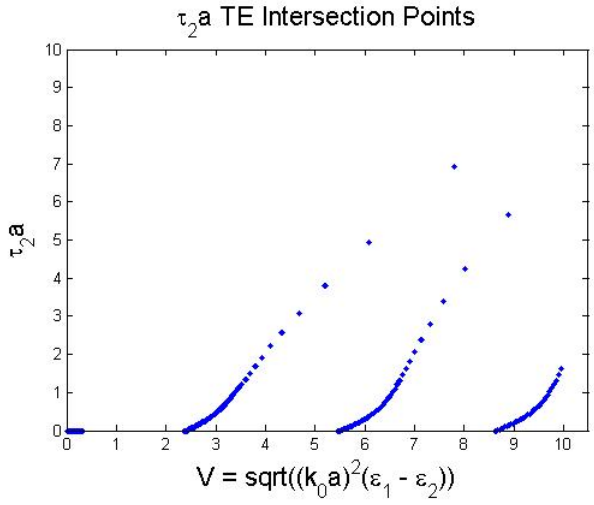

Figure 9: τ_2 TE Intersection Points with V parameter

The case where $W_0 = 0$ corresponds to TM modes, which can be solved for in terms of the cutoff wave numbers. In this case,

$$W_0 = (\frac{\epsilon_{r2} S_{a'b'}}{\tau_2 a} - \frac{R_{b'c'}}{R_{bc}} \frac{\epsilon_{r2}}{\tau_3 a} S_{a'b}) J_0(\xi_1 a) + (S_{ab'} - \frac{\epsilon_{r3}}{\epsilon_{r2}} \frac{\tau_2 a}{\tau_3 a} \frac{R_{b'c}}{R_{bc}} S_{ab}) \frac{\epsilon_{r1} J_0'(\xi_1 a)}{\xi_1 a} \tag{31}$$

This equation was then simplified using recursion relations and the quotient approximation mentioned above, and then used to determine relationships for the cutoff wave numbers. The resulting curve for the cutoff wave number of the core ξ_1 when plotted vs. τ_3 is shown below.

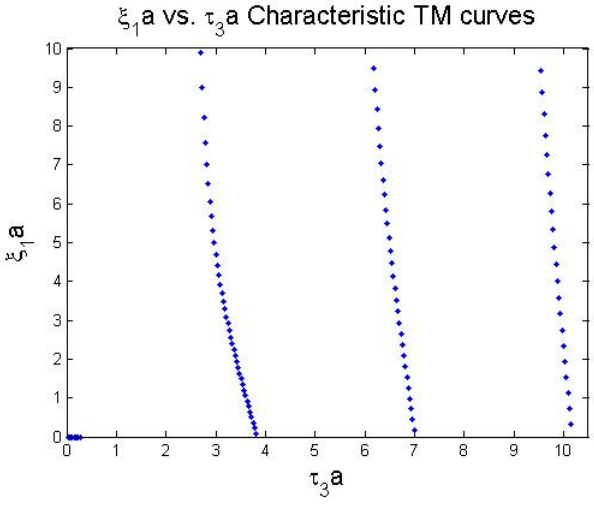

Figure 10: TM Characteristic Equation plot for ξ_1

In order for the Normalized Radius to correspond to the radius of a circle centered at the origin, it must be defined as $V = \sqrt{\xi_1^2 + \tau_3^2}$.

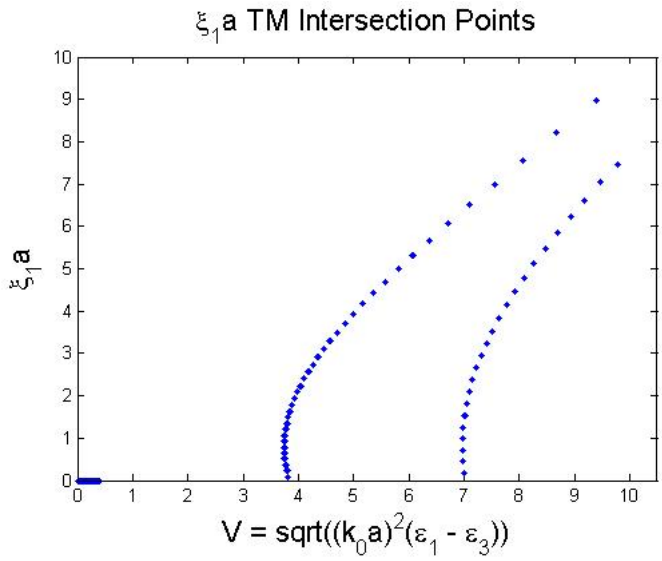

Figure 11: ξ_1 TE Intersection Points with V parameter

Like before, the TM Characteristic Equation can be used to solve for in terms of τ_2. The resulting plot is shown below in Figure 12.

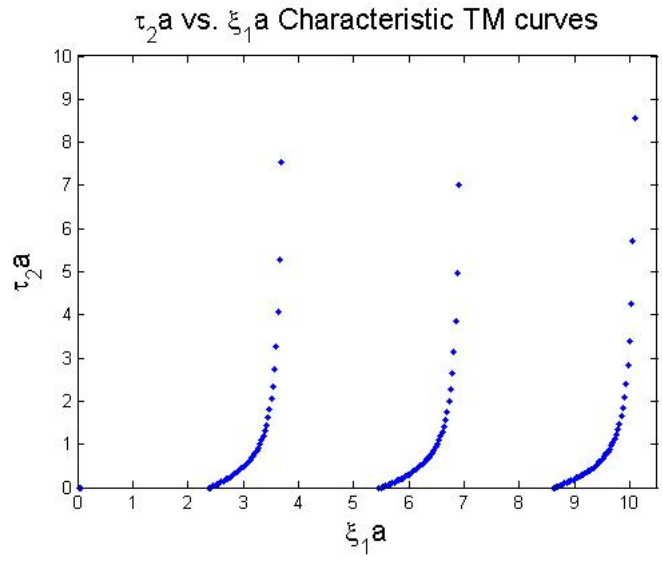

Figure 12: TM Characteristic Equation plot for τ_2

In this case, in order for the Normalized Radius to correspond to the radius of a circle centered at the origin, it must be defined as $V = \sqrt{\xi_1^2 + \tau_2^2}$. The resulting modal chart is plotted below. In terms of the dielectric permittivity of the layers, $V = \sqrt{(k_0 * a)^2(\epsilon_1 - \epsilon_2)}$.

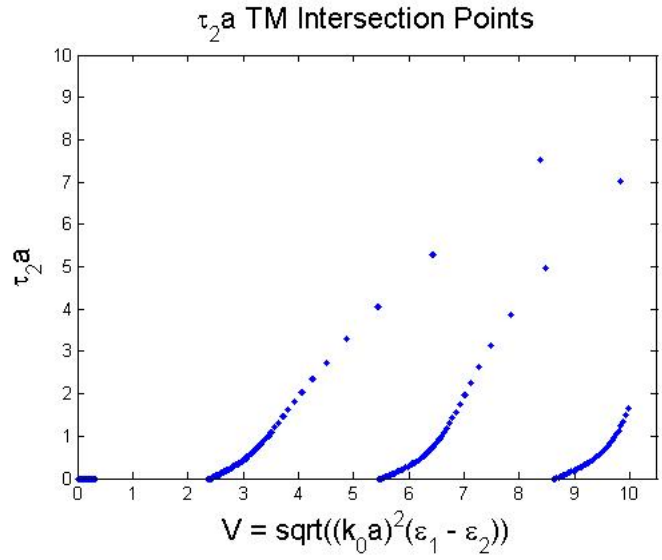

Figure 13: τ_2 TM Intersection Points with V parameter

In the above figures, the V-parameter is defined in terms of only two of the three cutoff wave numbers. While this form of definition is okay for two-layer fibers, for the three-layer fiber it is apparent that the complete dependence of the V-parameter on the cutoff wave numbers, and therefore the index variation and layer radius of all three layers, is not provided by this definition. The suggested approach for including in the complete dependence of the V-parameter is provided in the "Future Work" section.

5 DISCUSSION & SUMMARY

5.1 Discussion

In the previous section it had been mentioned that included within the characteristic functions T_ν, U_ν, V_ν and W_ν are various functions of Bessel functions that are not all well behaved in the limit that the radius of the outer layer c goes to infinity. Nonetheless, since these functions had appeared in quotient pairs, they had essentially been neglected, with the quotient set equal to -1. In terms of the cutoff wave numbers, the functions involved only the outer most layer with cutoff wave number τ_3. Due to this, when the characteristic equation was used to solve for τ_3, as was done for ξ_1 and τ_2 in the previous section, tangent function like curves in the first quadrant, as to be expected, did not appear. The curve that did appear is shown below.

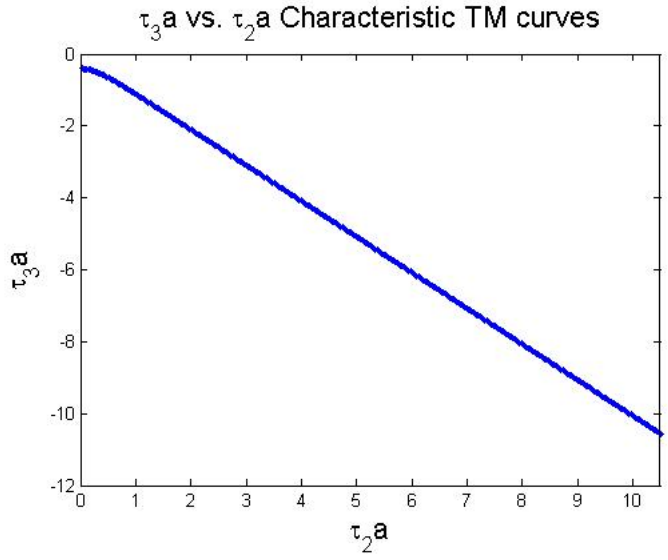

Figure 14: TM Characteristic Equation plot for τ_3

The reason that this occurred is likely due to the fact the by neglecting the aforementioned functioned resulted in disregarding some of the dependencies for τ_3.

While the resulting curves for ξ_1 and τ_2 do resemble what is to be expected, it is also apparent that since the solutions involve τ_3 the results cannot be completely accurate. Furthermore, when analyzing the data an interesting point becomes apparent. Consider the characteristic curves for the step index fiber, shown in Appendix A, and the τ_3 TM characteristic curve of Figure 14 above. In all the modes of both of these curves, the concavity can be found on the left side of the curve (the slope is increasing

upwards). However, for the ξ_1 TM and TE characteristic curves, the concavity is on the right side of the curve (the slope is increasing downwards). While it is possible that this attribute is the desired result, a more likely explanation involves the quotient of the poorly behaved functions that were set equal to -1. As mentioned above, setting the quotient this way is not always mathematically permissible. If in actuality the quotient would turn out to be a positive number, then the effect of negating it would lead to an inversion of the curve, as is observed.

5.2 Summary

The overall goal of this project was to determine what type of fiber is best suited for the propagation of light with Orbital Angular Momentum. The proposed method of achieving this goal was originally to learn how to use the method presented by Neves and Fernandes involving Frobenius and Taylor type solutions. If their results had been reproducible, subsequently the ability to generate mode profile plots for arbitrary fiber designs would follow. Unfortunately, this had not been the case, and in this regard the goal of the project was not achieved. Nevertheless, the project was successful in other respects. One of the goals for this project involved learning about light with Orbital Angular Momentum and its attributes. Through the research conducted in this MQP, this goal was achieved. Furthermore, by presenting what was learned to others, knowledge of this field was spread. A subsequent goal was the study of the ring fiber structure. Although the Neves and Fernandes approach proved to not be the best course of action, another approximate approach was found in its place. While the analysis was not completed to the point of determining the best waveguide mode profile for the propagation of OAM light, an analytic BVP approach was attempted, and an approximate solution was plotted and analyzed. The reason for studying this specific design is that the ring fiber seems appropriate for the propagation of light with OAM, which arises from the cylindrical Lauguere-Gaussian Modes. Aside from the mathematical analysis, the greatest success in this project came in the gaining of relevant research experience. Not only did the project involve the conducting of research to become familiar with a new topic, but also taught the hard learned lesson of the difficulties and unexpected outcomes that arise in real world research.

6 FUTURE WORK

While the research conducted in this project did not result in any significant findings, the methods presented can be used to further progress in the study of light with Orbital Angular Momentum and its propagation. Throughout the project, several approaches to solving the 3-layer fiber were attempted. Since some of these approaches proved to be more of a learning experience rather than a step toward the goal, the future researcher can avoid these attempts altogether. The recommended starting point for future work would be with the characteristic equation provided in the work by Lin and Zaki. In doing so, however, it must be stressed that unfounded assumptions must be avoided in order to have an accurate result. Therefore, rather than setting the quotient of a function that approaches infinity and on that approaches negative infinity to equal -1, as was done in this paper, a mathematical approach involving less assumptions must be taken. The recommended method would be an asymptotic analysis to determine the limiting behavior of each of the functions that are not well behaved, and then evaluating the quotient using finite values. Since the functions in this problem involve Bessel functions, a good starting place would be an asymptotic analysis of the Bessel functions involved.

Once this analysis is complete, the resulting terms in the characteristic equation would become accurate for the 3-layer fiber in the limit that the outer radius becomes infinitely large. The characteristic equation can then be used to create a three dimensional plot of the cutoff wave numbers of the medium, ξ_1, τ_2, and τ_3. In the analysis in this paper, only two of the cutoff wave numbers were plotted versus eachother at a time. Therefore, the V parameter was chosen to correspond to the arc of a circle on this plot, such that $x^2 + y^2 = V^2$, where x corresponds to the cutoff wave number on the x-axis and y corresponds to the cutoff wave number on the y-axis. However, using this method resulted in the dependence of the V-parameter to the third cutoff wave number to be omitted. Nevertheless, for the three dimensional case, the V-parameter would correspond to the surface of an ellipsoid which would incorporate the dependence of all three cutoff wave numbers. To see why it is an ellipsoid, rather than a sphere, recall the definitions of the cutoff wave numbers,

$$\xi_1 = \sqrt{k_1^2 - \beta^2} \quad , \tag{32}$$

$$\tau_2 = \sqrt{\beta^2 - k_2^2} \quad , \tag{33}$$

$$\tau_3 = \sqrt{\beta^2 - k_2^2} \quad . \tag{34}$$

By defining the V-parameter such that the β term cancels, it follows that

$$2\xi_1^2 + \tau_2^2 + \tau_3^2 = V^2 \quad , \tag{35}$$

which is the equation for an ellipsoid in the cutoff wave number space. The intersection points of the three dimensional cutoff wave number plot and the surface of this ellipsoid will correspond to the modal points of the fiber, which can then be plotted to create a modal profile plot.

7 WORK CITED

References

[1] L. Allen & M. Padgett, *The Poynting vector in Laguerre-Gaussian beams and the interpretation of their angular momentum density*, Optics Communications 184, 2000, pp. 67–71.

[2] Allen, L., M. Beijersbergen, R. Spreeuw, & J. Woerdman, *Orbital angular momentum of light and the transformation of Lauguerre-Gaussian laser modes*, Physical Review A, Volume 45, Number 11, 1992, pp. 8184–8189.

[3] Allen, L., M. J. Padgett and M. Babiker, *The Orbital Angular Momentum of Light*, Progress in Optics XXXIX, (Elsevier), 1999, pp. 291–369.

[4] Amol, Jain, *Creation of Optical Vortices Using an Adjustable Spiral*, Siemens-Westinghouse Competition, 2005.

[5] Bazhenov, V. Yu., M. V. Vasnetsov and M.S. Soskin, *Laser beams with screw dislocations in their wavefronts*, Jounal of Experimental and Theoretical Physics (Letters), 1990, pp. 429-431.

[6] Bozinovic, N., P. Kristensen and S. Ramachandran, *Are Orbital Angular Momentum (OAM/Vortex) States of Light Long-Lived in Fibers?*, Technical Digest, 2011, pp. 1–3.

[7] Bozinovic, N., P. Kristensen and S. Ramachandran. *Long-range fiber-transmission of photons with orbital angular momentum*, OSA/CLEO, 2011.

[8] Carpentier, Alicia V., Humberto Michinel and and José R. Salgueiro, *Making optical vortices with computer-generated holograms*, American Journal of Physics, 2008 pp. 916–920.

[9] Crawford, Patrick, et al, *Light Beams in High Order Modes*, Physical Review Letters (PRL 90), 2003.

[10] Harris, M., C. A. Hills and J. M. Vaughan, *Optical helices and spiral interference fringes*, Optics Communications 106, 1993, pp. 129–133.

[11] Iizuka, Keigo, *Elements of Photonics Vol. II For Fibers and Integrated Optics*, New York, NY, Wiley & Sons, INC, 2002.

[12] Kumar, Ranjeet, et al, *Generation and detection of optical vortices using all fiber-optic system*, Optics Communications 281, 2008, pp. 3414–3420.

[13] Leach, Jonathan, Miles. J. Padgett and Stephen M. Barnett, *Measuring the Orbital Angular Momentum of a Single Photon*, Physical Review Letters Vol. 88, No. 25, 2002, pp. 1–4.

[14] Lin, Hongchin and Zaki, K. A., *Properties of Three-layer Dielectric Loaded Waveguides*, IEEE Transactions on Magnetics, Vol. 25, No. 4, 2006.

[15] Lindley, David, *Focus: Giving light a new twist*, Phyics Review Focus, Vol. 17, No. 15, 2006.

[16] Marrucci, L., C. Manzo and D. Papro, *Optical Spin-to-Orbital Angular Momentum Conversion in Inhomogeneous Anistropic Media*, Physical Review Letters, 2006, pp. 1–4.

[17] Minkel, J. R., *Focus: Breaking Free of Bits*, Phyics Review Focus Vol. 9, No. 29, 2002.

[18] Nam, Hannarae Annie and Choate Rosemary Hall, *Creating a Robust Optical Vortex Beam with a Single Cylinder Lens*, Intel Science Talent Search, 2010.

[19] Neves, I. V. and A. S. C. Fernandes, *Modal Characteristics for A-type and V-type Dielectric Profile Fibers*, Microwave and Optical Technology Letters Vol. 16, No. 11, 1997, pp. 164–169.

[20] Neves, I. V. and A. S. C. Fernandes, *Modal Characteristics for W-type and M-type Dielectric Profile Fibers*, Microwave and Optical Technology Letters Vol. 22, No. 6, 1999, pp. 398–405.

[21] Neves, I. V. and A. S. C. Fernandes, *Wave Propagation in a Radially Inhomogeneous Cylindrical Dielectric Structure: A General Analytical Solution*, Microwave and Optical Technology Letters Vol. 5, No. 15, 1992, pp. 675–679.

[22] Padgett, M. and L. Allen, *Light with a twist in it tail*, Contemporary Physics Vol. 41, No. 5, 2000, pp. 275–285.

[23] Padgett, M. J., et al, *An experiment to observe the intensity and phase structure of Laguerre-Gaussian laser modes*, American Journal of Physics 64, 1996, pp. 77–82.

[24] Ramachandran, Siddharth, Poul Kristensen and Man F. Yan, *Generation and propagation of radially polarized beams in optical fibers*, Optics Letters Vol. 34, No. 16, 2009, pp. 2525–2527.

[25] Sacks, Z. S., D. Rozas and G. A. Swartzlander Jr., *Holographic formation of optical-vortex filaments*, Journal of the Optical Society of America B Vol. 15, No.8, 1998, pp. 2226–2233.

[26] Yue, Yang, et al., *Mode Properties and Propagation Effects of Optical Orbital Angular Momentum (OAM) Modes in a Ring Fiber*, IEEE Photonics Journal Vol 4, No. 2, 2012, pp. 535–543.

8 APPENDICES

8.1 Appendix A: Solution of Step-Index Fiber BVP

Presented in this section is an analysis of the modes of a waveguide, beginning by solving Maxwell's equations for a general waveguide, with a step-index fiber in mind, following the method presented by Izuka in Elements of Photonics V.II. The geometry of an optical fiber is cylindrical, so the most natural coordinate system to use are the cylidrical coordinates in the proceeding argument, where the coordinates ρ will be use to represent the radial axis, ϕ will be used to represent the azimuthal angle, and z will be used to represent the longitudinal axis.

8.1.1 Discussion

The first step that must be taken is finding the solution to the vectorial wave equations

$$\nabla^2\mathbf{E} + (nk)^2\mathbf{E} = 0 \quad , \tag{1}$$

where $\mathbf{E}$ represents the electric field vector (E_ρ, E_ϕ, E_z), and

$$\nabla^2\mathbf{H} + (nk)^2\mathbf{H} = 0 \quad , \tag{2}$$

where $\mathbf{H}$ represents the electric field vector (H_ρ, H_ϕ, H_z). In both these case, k is the wave number, and n refers to an index number related to the relative permeabilty of a medium by the relation

$$n^2 = \epsilon_r \quad . \tag{3}$$

As different materials have different permeabilities, it is clear that if the optical fiber is made out of layers of different materials then the corresponding index number will be used for each material. Therefore, the following convention will be used: For a material with N layers, n_i will refer to the index number of the i^{th} layer, for $i = 1, 2...N$, where 1 refers to the inner most, or core, layer. The simplest case is the step idex fiber, with just core (n_1) and cladding (n_2) layers $(N = 2)$.

In cylidrical cooridnates, the Laplacian operator ∇^2 takes the form

$$\nabla^2 = \frac{1}{\rho}\frac{\partial}{\partial\rho}\left(\rho\frac{\partial}{\partial\rho}\right) + \frac{1}{\rho^2}\frac{\partial^2}{\partial\phi^2} + \frac{\partial^2}{\partial z^2} \quad . \tag{4}$$

Thus Eq. (1) becomes

$$\nabla^2\mathbf{E} + (nk)^2\mathbf{E} = \frac{1}{\rho}\frac{\partial}{\partial\rho}\left(\rho\frac{\partial\mathbf{E}}{\partial\rho}\right) + \frac{1}{\rho^2}\frac{\partial^2\mathbf{E}}{\partial\phi^2} + \frac{\partial^2\mathbf{E}}{\partial z^2} + (nk)^2\mathbf{E} = 0 \quad . \tag{5}$$

Similarly, Eq. (2) becomes

$$\nabla^2\mathbf{H} + (nk)^2\mathbf{H} = \frac{1}{\rho}\frac{\partial}{\partial\rho}\left(\rho\frac{\partial\mathbf{H}}{\partial\rho}\right) + \frac{1}{\rho^2}\frac{\partial^2\mathbf{H}}{\partial\phi^2} + \frac{\partial^2\mathbf{H}}{\partial z^2} + (nk)^2\mathbf{H} = 0 \quad . \tag{6}$$

We may proceed by first concidering only the longitudinal component of the electric field.

$$\nabla^2 E_z + (nk)^2 E_z = \frac{1}{\rho}\frac{\partial}{\partial\rho}\left(\rho\frac{\partial E_z}{\partial\rho}\right) + \frac{1}{\rho^2}\frac{\partial^2 E_z}{\partial\phi^2} + \frac{\partial^2 E_z}{\partial z^2} + (nk)^2 E_z = 0 \quad . \tag{7}$$

This equation may be solved by the method of separation of variables, where we assume that E_z is the product of three independent functions of each coordinate,

$$E_z = R(\rho)\Phi(\phi)Z(z) = R\Phi Z \quad . \tag{8}$$

In this context, Eq. (7) becomes

$$\nabla^2 R\Phi Z + (nk)^2 R\Phi Z = \frac{1}{\rho}\frac{\partial}{\partial\rho}\left(\rho\frac{\partial R\Phi Z}{\partial\rho}\right) + \frac{1}{\rho^2}\frac{\partial^2 R\Phi Z}{\partial\phi^2} + \frac{\partial^2 R\Phi Z}{\partial z^2} + (nk)^2 R\Phi Z \tag{9}$$

$$= R''\Phi Z + \frac{1}{\rho}R'\Phi Z + \frac{1}{\rho^2}R\Phi'' Z + R\Phi Z'' + (nk)^2 R\Phi Z = 0 \quad . \tag{10}$$

Dividing Eq. (10) by $R\Phi Z$ gives

$$\frac{R''}{R} + \frac{R'}{\rho R} + \frac{\Phi''}{\rho^2\Phi} + \frac{Z''}{Z} + (nk)^2 = 0 \quad , \tag{11}$$

or

$$\frac{R''}{R} + \frac{R'}{\rho R} + \frac{\Phi''}{\rho^2\Phi} + (nk)^2 = -\frac{Z''}{Z} = \beta^2 \quad , \tag{12}$$

where β is a yet to be determined. Writing the equation in this manner is possible because the LHS of Eq. (12) is a function of only ρ and ϕ, while $-Z''/Z$ is a function of only z. The only way for these two terms to be equal would be if they were both constant. It follows from $-\frac{Z''}{Z} = \beta^2$ that

$$Z'' + \beta^2 Z = 0 \quad , \tag{13}$$

which has a solution of the form

$$Z(z) = Ae^{j\beta z} + Be^{-j\beta z} \quad , \tag{14}$$

where A & B are yet to be determined constant coefficients, and $j = \sqrt{-1}$. The same method can be used to find $R(\rho)$ and $\Phi(\phi)$ by writing Eq. (12) as

$$\frac{R''}{R} + \frac{R'}{\rho R} + \frac{\Phi''}{\rho^2 \Phi} + (nk)^2 - \beta^2 = 0 \quad , \tag{15}$$

and then multiplying by ρ^2 to give

$$\rho^2 \frac{R''}{R} + \rho \frac{R'}{R} + \rho^2((nk)^2 - \beta^2) + \frac{\Phi''}{\Phi} = 0 \quad , \tag{16}$$

and recognizing that, in order for this to be true, we must have

$$\rho^2 \frac{R''}{R} + \rho \frac{R'}{R} + \rho^2((nk)^2 - \beta^2) = -\frac{\Phi''}{\Phi} = \nu^2 \quad . \tag{17}$$

where ν is a yet to be determined. It follows from $-\frac{\Phi''}{\Phi} = \nu^2$ that

$$\Phi'' + \nu^2 \Phi = 0 \quad , \tag{18}$$

which has a solution of the form

$$\Phi(\phi) = Ce^{j\nu\phi} + De^{-j\nu\phi} \quad , \tag{19}$$

where C & D are yet to be determined constant coefficients. The remaining equation is

$$\rho^2 \frac{R''}{R} + \rho \frac{R'}{R} + \rho^2((nk)^2 - \beta^2) = \nu^2 \quad , \tag{20}$$

which may be rearranged in the form of the Bessel Equation,

$$\rho^2 R'' + \rho R' + (\rho^2((nk)^2 - \beta^2) - \nu^2)R = 0 \quad . \tag{21}$$

Before proceeding in writing a solution in terms of Bessel functions, some care must be taken due to the term $((nk)^2 - \beta^2)$, which may be either a positive or negative quanitity. Therefore, let us introduce the terms κ and γ such that

$$(nk)^2 - \beta^2 = \kappa^2 = -\gamma^2 \quad . \tag{22}$$

If we take $((nk)^2 - \beta^2)$ to be positive, then Eq. (21) has a solution of the form

$$R(\rho) = EJ_\nu(\kappa\rho) + GN_\nu(\kappa\rho) \quad , \tag{23}$$

where E & G are yet to be determined constant coefficients, and $J_\nu(K\rho)$ & $N_\nu(K\rho)$ are Bessel functions of the first and second kinds, respectively, of order ν. If we take $((nk)^2 - \beta^2)$ to be negative, then Eq. (21) has a solution of the form

$$R(\rho) = HI_\nu(\gamma\rho) + FK_\nu(\gamma\rho) \quad , \tag{24}$$

where H & F are yet to be determined constant coefficients, and $I_\nu(\gamma\rho)$ & $K_\nu(\gamma\rho)$ are the modified Bessel functions of the first and second kinds, respectively, of order ν. The most immediate property of the Bessel functions that will be of concern are as follows:

$$\lim_{\rho\to\infty} I_\nu = \infty \quad , \tag{25}$$

$$\lim_{\rho\to 0} N_\nu = \lim_{\rho\to 0} K_\nu = \infty \quad . \tag{26}$$

In order to determine whether to use Eq. (23), Eq. (24), or a combination of the two, first consider the simplest case of a step idex fiber, with core index n_1 and cladding index n_2. Inside the core, the term $((nk)^2 - \beta^2)$ is a positive quantity,

$$(n_1 k)^2 - \beta^2 = \kappa^2 \quad , \tag{27}$$

which hints at the use of Eq. (23) with $G = 0$, from Eq. (26), since we are only concerned with physical solutions that converge. In the cladding, the term $((nk)^2 - \beta^2)$ is a negative quantity,

$$(n_2 k)^2 - \beta^2 = -\gamma^2 \quad , \tag{28}$$

which hints at the use of Eq. (24) with $H = 0$, from Eq. (25), since we are only concerned with physical solutions that converge. Therefore, we may infer a solution of the form

$$R(\rho) = EJ_\nu(\kappa\rho) + FK_\nu(\gamma\rho) \tag{29}$$

for a step index fiber. However, it must be noted that for an arbitrary fiber with regions that do not include $\rho = 0$ or $\rho = \infty$, both terms in equations (23) and (24) must be included in the analysis. The values of ν determine the different modes of the Bessel functions. The curves for varying values of ν for

the Ordinary Bessel Function of the First Kind, as a function of $\kappa\rho$, is shown below.

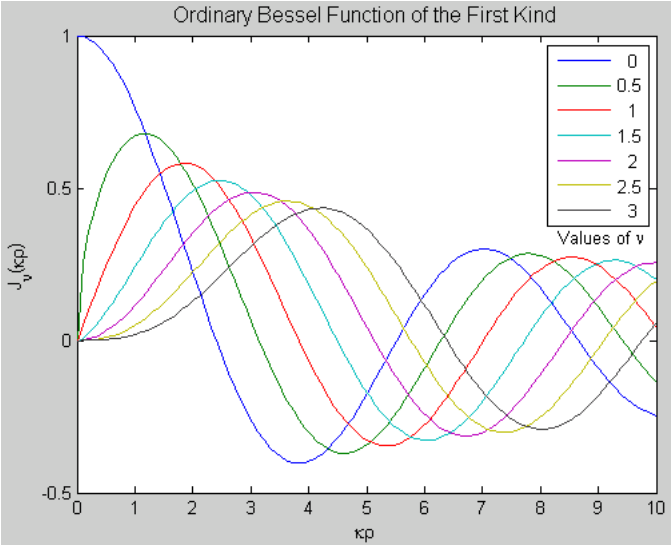

The curves for varying values of ν for the Modified Bessel Function of the Second Kind, as a function of $\gamma\rho$ is shown below. It is apparent that the function blows up at $\rho = 0$, justifying Eq. (26).

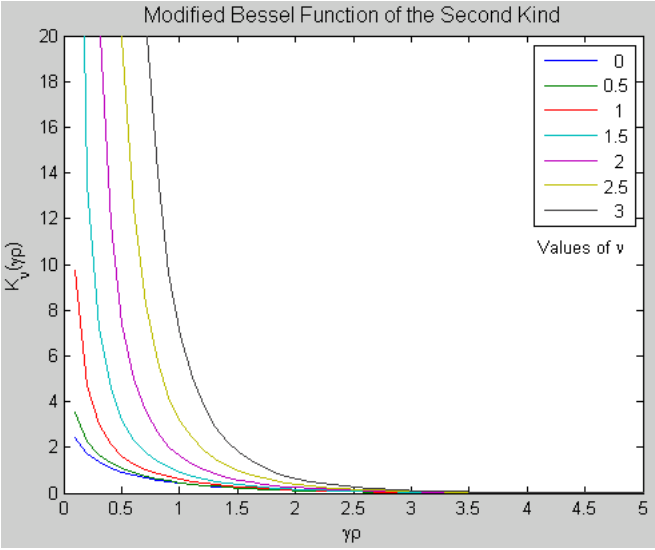

Thus, since $E_z = R(\rho)\Phi(\phi)Z(z)$, we conclude

$$E_z = \Big(EJ_\nu(\kappa\rho) + FK_\nu(\gamma\rho)\Big)\Big(Ce^{j\nu\phi} + De^{-j\nu\phi}\Big)\Big(Ae^{j\beta z} + Be^{-j\beta z}\Big) \quad . \tag{30}$$

This result may be simplified by considering only azimuthal rotation in one direction, so $\Phi(\phi) \to e^{j\nu\phi}$. Furthermore, since the function Z(z) deals with the longitudinal propagation of the wave, we may limit the consideration to only one direction, $Z(z) \to e^{j\beta z}$. Finally, by realizing that the constant coefficients

are arbitrary, and may be combined to give new constant coefficients, we may write

$$E_z = \Big(AJ_\nu(\kappa\rho) + BK_\nu(\gamma\rho) \Big) e^{j\nu\phi} e^{j\beta z} \quad , \tag{31}$$

where A & B are new constant coefficients, that are yet to be determined. It is apparent that the same argument could have been made for the ϕ and z-components of the magnetic field, H_z. With this in mind, we can conclude

$$H_z = \Big(CJ_\nu(\kappa\rho) + DK_\nu(\gamma\rho) \Big) e^{j\nu\phi} e^{j\beta z} \quad , \tag{32}$$

where C & D are new constant coefficients, that are yet to be determined. Note that for a step/–index fiber, A & C are non-zero in the core region but are 0 in the cladding region. Similarly, B & D are non-zero in the cladding region but are 0 in the core region.

To find the remaining components of the electric and magnetic fields, Maxwell's Equations must be used, or more specifically, Faraday's Law

$$\nabla \times \mathbf{E} = -\mu \frac{\partial \mathbf{H}}{\partial t} \quad , \tag{33}$$

and Ampère's Law

$$\nabla \times \mathbf{H} = \epsilon \frac{\partial \mathbf{E}}{\partial t} \quad . \tag{34}$$

The time dependence of the electric and magnetic fields can be written explicity as

$$\mathbf{E}(\rho, \phi, z, t) = \mathbf{E}(\rho, \phi, z) e^{-j\omega t} \quad , \tag{35}$$

$$\mathbf{H}(\rho, \phi, z, t) = \mathbf{H}(\rho, \phi, z) e^{-j\omega t} \quad , \tag{36}$$

where ω is the corresponding angular velocity, related to the wave number k by the formula

$$(nk)^2 = \omega^2 \mu\epsilon \quad . \tag{37}$$

Therefore, Eqs. (33) & (34) respectively take the forms

$$\nabla \times \mathbf{E} = j\omega\mu\mathbf{H} \quad , \tag{38}$$

$$\nabla \times \mathbf{H} = -j\omega\epsilon\mathbf{E} \quad . \tag{39}$$

Eq. (38) results in the three equations

$$\frac{1}{\rho}\frac{\partial E_z}{\partial \phi} - \frac{\partial E_\phi}{\partial z} = j\omega\mu H_\rho \quad , \tag{40}$$

$$\frac{\partial E_\rho}{\partial z} - \frac{\partial E_z}{\partial \rho} = j\omega\mu H_\phi \quad , \tag{41}$$

$$\frac{1}{\rho}\frac{\partial(\rho E_\phi)}{\partial \rho} - \frac{1}{\rho}\frac{\partial E_\rho}{\partial \phi} = j\omega\mu H_z \quad . \tag{42}$$

Eq. (39) results in the three equations

$$\frac{1}{\rho}\frac{\partial H_z}{\partial \phi} - \frac{\partial H_\phi}{\partial z} = -j\omega\epsilon E_\rho \quad , \tag{43}$$

$$\frac{\partial H_\rho}{\partial z} - \frac{\partial H_z}{\partial \rho} = -j\omega\epsilon E_\phi \quad , \tag{44}$$

$$\frac{1}{\rho}\frac{\partial(\rho H_\phi)}{\partial \rho} - \frac{1}{\rho}\frac{\partial H_\rho}{\partial \phi} = -j\omega\epsilon E_z \quad . \tag{45}$$

For notational simplification in solving these equations, recall the form for E_z,

$$E_z = R(\rho)\Phi(\phi)Z(z) = R\Phi Z \quad , \tag{46}$$

where

$$R(\rho) = R = \Big(AJ_\nu(\kappa\rho) + BK_\nu(\gamma\rho)\Big) \quad , \tag{47}$$

$$\Phi(\phi) = \Phi = e^{j\nu\phi} \quad , \tag{48}$$

$$Z(z) = Z = e^{j\beta z} \quad . \tag{49}$$

In solving for each component in Maxwell's equations, it will be necessary to take partial derivatives for each of the above terms. The partial of R with respect to ρ is

$$\frac{\partial R(\rho)}{\partial \rho} = M(\rho) = \left[\frac{A\kappa}{2}\Big(J_{\nu-1}(\kappa\rho) - J_{\nu+1}(\kappa\rho)\Big) - \frac{B\gamma}{2}\Big(K_{\nu-1}(\gamma\rho) + K_{\nu+1}(\gamma\rho)\Big)\right] \quad , \tag{50}$$

where the respective recursion relations for the Bessel functions were used, and M was defined for future

convenience. The remaining two partial derivatives are

$$\frac{\partial \Phi(\phi)}{\partial \phi} = j\nu e^{j\nu\phi} = j\nu\Phi \quad , \tag{51}$$

$$\frac{\partial Z(z)}{\partial z} = j\beta e^{j\beta z} = j\beta Z \quad . \tag{52}$$

Eqs. (51) and (52) reveal the apparent simplifications,

$$\frac{\partial}{\partial \phi} = j\nu \quad \text{and} \quad \frac{\partial}{\partial z} = j\beta \quad . \tag{53}$$

Furthermore, let us label the analog of $R(\rho)$ in the magnetic field equation as $P(\rho) = P = \Big(CJ_\nu(\kappa\rho) + DK_\nu(\gamma\rho)\Big)$. We may now write out Eqs. (41) and (43) explicity to solve for E_ρ and H_ϕ. Eq. (41) becomes

$$\frac{\partial E_\rho}{\partial z} - \frac{\partial E_z}{\partial \rho} = j\omega\mu H_\phi \quad . \tag{54}$$

$$j\beta E_\rho - M\Phi Z = j\omega\mu H_\phi \quad . \tag{55}$$

Solving for H_ϕ results in

$$H_\phi = \frac{j\beta E_\rho - M\Phi Z}{j\omega\mu} \quad . \tag{56}$$

Likewise, Eq. (43) becomes

$$\frac{1}{\rho}\frac{\partial H_z}{\partial \phi} - \frac{\partial H_\phi}{\partial z} = -j\omega\epsilon E_\rho \quad . \tag{57}$$

$$\frac{j\nu}{\rho} P\Phi Z - j\beta H_\phi = -j\omega\epsilon E_\rho \quad . \tag{58}$$

Solving for H_ϕ results in

$$H_\phi = \frac{j\omega\epsilon E_\rho + \frac{j\nu}{\rho} P\Phi Z}{j\beta} \quad . \tag{59}$$

Therefore,

$$\frac{j\beta E_\rho - M\Phi Z}{j\omega\mu} = \frac{j\omega\epsilon E_\rho + \frac{j\nu}{\rho} P\Phi Z}{j\beta} \quad , \tag{60}$$

which may be solved for E_ρ to give

$$E_\rho = \frac{(\beta M + \frac{j\omega\mu\nu}{\rho} P)\Phi Z}{j(\beta^2 - \mu\omega^2\epsilon)} \quad . \tag{61}$$

This solution may then be substituted into either Eq. (56) or Eq. (59) to give

$$H_\phi = \frac{(\omega\epsilon M + \frac{j\beta\nu}{\rho}P)\Phi Z}{j(\beta^2 - \mu\omega^2\epsilon)} \quad . \tag{62}$$

Similarly, Eqs. (40) and (44) can be solved to give E_ϕ and H_ρ. This is done by first noting that

$$\frac{\partial P(\rho)}{\partial \rho} = N(\rho) = \left[\frac{C\kappa}{2}\Big(J_{\nu-1}(\kappa\rho) - J_{\nu+1}(\kappa\rho)\Big) - \frac{D\gamma}{2}\Big(K_{\nu-1}(\gamma\rho) + K_{\nu+1}(\gamma\rho)\Big)\right] \quad . \tag{63}$$

Therefore, the azimuthal component of the electric field is

$$E_\phi = \frac{(\frac{j\beta\nu}{\rho}R - \omega\mu N)\Phi Z}{j(\beta^2 - \mu\omega^2\epsilon)} \quad , \tag{64}$$

and the radial component of the magnetic field is

$$H_\rho = \frac{(-\frac{j\omega\epsilon\nu}{\rho}R + \beta N)\Phi Z}{j(\beta^2 - \mu\omega^2\epsilon)} \quad . \tag{65}$$

8.1.2 Characteristic Equation

By applying the boundary condition that the tangential compontents of the electric field (E_z and E_ϕ) and magnetic field (H_z and H_ϕ) must be continuous at the boundary between regions, we may find the Characteristic Equation of the optical fiber. First, let us consider a step-index fiber with the boundary between the core and cladding regions at $\rho = a$. The z-component of the Electric Field in the two regions are

$$E_z(\rho < a) = AJ_\nu(\kappa\rho)e^{j\nu\phi}e^{j\beta z} \quad , \tag{66}$$

$$E_z(\rho > a) = BK_\nu(\gamma\rho)e^{j\nu\phi}e^{j\beta z} \quad . \tag{67}$$

At the boundary

$$E_z(\rho = a) = AJ_\nu(\kappa a)e^{j\nu\phi}e^{j\beta z} = BK_\nu(\gamma a)e^{j\nu\phi}e^{j\beta z} \quad , \tag{68}$$

from which we can solve for one coefficient in terms of the other

$$B = A\frac{J_\nu(\kappa a)e^{j\nu\phi}e^{j\beta z}}{K_\nu(\gamma a)e^{j\nu\phi}e^{j\beta z}} = A\frac{J_\nu(\kappa a)}{K_\nu(\gamma a)} \quad . \tag{69}$$

Similarly, the z-component of the Magnetic Field in the two regions are

$$H_z(\rho < a) = CJ_\nu(\kappa\rho)e^{j\nu\phi}e^{j\beta z} \quad , \tag{70}$$

$$H_z(\rho > a) = DK_\nu(\gamma\rho)e^{j\nu\phi}e^{j\beta z} \quad . \tag{71}$$

At the boundary

$$E_z(\rho = a) = CJ_\nu(\kappa a)e^{j\nu\phi}e^{j\beta z} = DK_\nu(\gamma a)e^{j\nu\phi}e^{j\beta z} \quad , \tag{72}$$

from which we can solve for one coefficient in terms of the other

$$D = C\frac{J_\nu(\kappa a)e^{j\nu\phi}e^{j\beta z}}{K_\nu(\gamma a)e^{j\nu\phi}e^{j\beta z}} = C\frac{J_\nu(\kappa a)}{K_\nu(\gamma a)} \quad . \tag{73}$$

Since we have determined the relationship between coefficients, we may write out the ϕ-components of the Electric and Magnetic Fields each in terms of one unknown coefficient, which we will ideally be able to cancel out. The ϕ-component of the Electric Field in the two regions are

$$E_\phi = \frac{(\frac{j\beta\nu}{\rho}R - \omega\mu N)\Phi Z}{j(\beta^2 - \mu\omega^2\epsilon)} \quad , \tag{74}$$

$$E_\phi(\rho < a) = \frac{\left[\frac{j\beta\nu}{\rho}AJ_\nu(\kappa\rho) - \omega\mu\frac{C\kappa}{2}\Big(J_{\nu-1}(\kappa\rho) - J_{\nu+1}(\kappa\rho)\Big)\right]\Phi Z}{j(\beta^2 - \mu\omega^2\epsilon)} \quad , \tag{75}$$

$$E_\phi(\rho > a) = \frac{\left[\frac{j\beta\nu}{\rho}BK_\nu(\gamma\rho) + \omega\mu\frac{D\gamma}{2}\Big(K_{\nu-1}(\gamma\rho) + K_{\nu+1}(\gamma\rho)\Big)\right]\Phi Z}{j(\beta^2 - \mu\omega^2\epsilon)} \quad . \tag{76}$$

To reduce the amount of space taken, let us denote the derivatives

$$\frac{J_{\nu-1}(\kappa\rho) - J_{\nu+1}(\kappa\rho)}{2} = J_\nu^{'} \quad , \tag{77}$$

$$\frac{-(K_{\nu-1}(\gamma\rho) + K_{\nu+1}(\gamma\rho))}{2} = K_\nu^{'} \quad . \tag{78}$$

Equating the equations (75) and (76) at the boundary $\rho = a$, and rearranging after a bit of mathematical manipulation gives

$$A\beta\nu\left(\frac{1}{(\kappa a)^2} + \frac{1}{(\gamma a)^2}\right) + jB\omega\mu\left(\frac{J_\nu^{'}(\kappa a)}{\kappa a J_\nu(\kappa a)} + \frac{K_\nu^{'}(\gamma a)}{\gamma a K_\nu(\gamma a)}\right) = 0 \quad . \tag{79}$$

Following a similar argument for the ϕ-component of the Magnetic Field leads to the equation

$$A\omega\left(\frac{\epsilon_1 J_\nu^{'}(\kappa a)}{\kappa a J_\nu(\kappa a)}+\frac{\epsilon_2 K_\nu^{'}(\gamma a)}{\gamma a K_\nu(\gamma a)}\right)+jB\beta\nu\left(\frac{1}{(\kappa a)^2}+\frac{1}{(\gamma a)^2}\right)=0 \quad . \tag{80}$$

The characteristic equation is found by taking the determinite of the coefficients of A and B in equations (79) and (80), which must equal zero for nontrivial solutions of A and B.

$$det\begin{bmatrix} \beta\nu\left(\frac{1}{(\kappa a)^2}+\frac{1}{(\gamma a)^2}\right) & j\omega\mu\left(\frac{J_\nu^{'}(\kappa a)}{\kappa a J_\nu(\kappa a)}+\frac{K_\nu^{'}(\gamma a)}{\gamma a K_\nu(\gamma a)}\right) \\ \omega\left(\frac{\epsilon_1 J_\nu^{'}(\kappa a)}{\kappa a J_\nu(\kappa a)}+\frac{\epsilon_2 K_\nu^{'}(\gamma a)}{\gamma a K_\nu(\gamma a)}\right) & j\beta\nu\left(\frac{1}{(\kappa a)^2}+\frac{1}{(\gamma a)^2}\right)=0 \end{bmatrix}=0 \quad . \tag{81}$$

In evaluating the determinite, let us introduce the following terms for simplification:

$$\xi=\left(\frac{1}{(\kappa a)^2}+\frac{1}{(\gamma a)^2}\right) \quad , \tag{82}$$

$$\mathcal{J}=\frac{J_\nu^{'}(\kappa a)}{\kappa a J_\nu(\kappa a)} \quad , \tag{83}$$

$$\mathcal{K}=\frac{K_\nu^{'}(\gamma a)}{\gamma a K_\nu(\gamma a)} \quad . \tag{84}$$

Thus, the determinite

$$det\begin{bmatrix} \beta\nu\xi & j\omega\mu(\mathcal{J}+\mathcal{K}) \\ \omega(\epsilon_1\mathcal{J}+\epsilon_2\mathcal{K}) & j\beta\nu\xi=0 \end{bmatrix}=0 \quad , \tag{85}$$

$$=j\beta^2\nu^2\xi^2-j\omega^2\mu(\mathcal{J}+\mathcal{K})(\epsilon_1\mathcal{J}+\epsilon_2\mathcal{K})=0 \quad , \tag{86}$$

$$=\beta^2\nu^2\xi^2-\omega^2\mu\epsilon_1(\mathcal{J}+\mathcal{K})(\mathcal{J}+\frac{\epsilon_2}{\epsilon_1}\mathcal{K})=0 \quad , \tag{87}$$

$$=\beta^2\nu^2\xi^2-(n_1k)^2(\mathcal{J}+\mathcal{K})(\mathcal{J}+\left(\frac{n_2}{n_1}\right)^2\mathcal{K})=0 \quad . \tag{88}$$

Finally, after some slight rearrangement and reinserting the values from equations (82) to (84), the resulting general characteristic equation for a step-index fiber is

$$\left(\frac{1}{\kappa a}\frac{J_\nu'(\kappa a)}{J_\nu(\kappa a)}+\frac{1}{\gamma a}\frac{K_\nu'(\gamma a)}{K_\nu(\gamma a)}\right)\left(\frac{1}{\kappa a}\frac{J_\nu'(\kappa a)}{J_\nu(\kappa a)}+\left(\frac{n_2}{n_1}\right)^2\frac{1}{\gamma a}\frac{K_\nu'(\gamma a)}{K_\nu(\gamma a)}\right)=\left[\frac{\beta\nu}{n_1k}\left(\frac{1}{(\kappa a)^2}+\frac{1}{(\gamma a)^2}\right)\right]^2 \quad . \tag{89}$$

Since the Bessel functions in the characteristic equation are of the order ν, the values for ν determine different types of modes of the optical fiber. The simplest case is when $\nu=0$, which are known as the Meridional Modes, since the azimuthal components of the Electric and Magnetic Fields are constant. In

this case we can apply the recursion relation

$$J_0'(\kappa a) = -J_1(\kappa a) \quad , \tag{90}$$

$$K_0'(\gamma a) - K_1(\gamma a) \quad . \tag{91}$$

The characteristic equation reduces to

$$\left(\frac{1}{\kappa a}\frac{J_1(\kappa a)}{J_0(\kappa a)} + \frac{1}{\gamma a}\frac{K_1(\gamma a)}{K_0(\gamma a)}\right)\left(\frac{1}{\kappa a}\frac{J_1(\kappa a)}{J_0(\kappa a)} + \left(\frac{n_2}{n_1}\right)^2\frac{1}{\gamma a}\frac{K_1(\gamma a)}{K_0(\gamma a)}\right) = 0 \quad . \tag{92}$$

In order for this to be true, either of the terms in the large parentheses in the characteristic equation must be equal to 0. Setting the first term to 0 corresponds to the Transverse Electric (TE) Modes

$$\frac{J_1(\kappa a)}{\kappa a J_0(Ka)} + \frac{K_1(\gamma a)}{\gamma a K_0(\gamma a)} = 0 \quad . \tag{93}$$

These modes are named in this manner because setting the above term to 0 causes the coefficient of the longitudinal component of the Electric Field to vanish. Therefore, $E_z \to 0$. Hence, only the transverse components of the Electric Field remain. In order to plot these modes, a physical parameter called the normalized radius V must be introduced,

$$V = ka\sqrt{n_1^2 - n_2^2} \quad , \tag{94}$$

which is used to relate the hereto unknown terms κa and γa,

$$V^2 = (\kappa a)^2 + (\gamma a)^2 \quad . \tag{95}$$

Shown in the figure below is a plot of the resulting TE modes, the dashed blue lines. The solid black line represents the arc from the origin to the normalized radius; thus the intersections of the modes and this arc corresponds to physical values. The solid red lines correspond to the zeroes of the J_0 Bessel function, while the solid purple lines correspond to the zeroes of the J_1 Bessel function, which serve as a boundary for the modes.

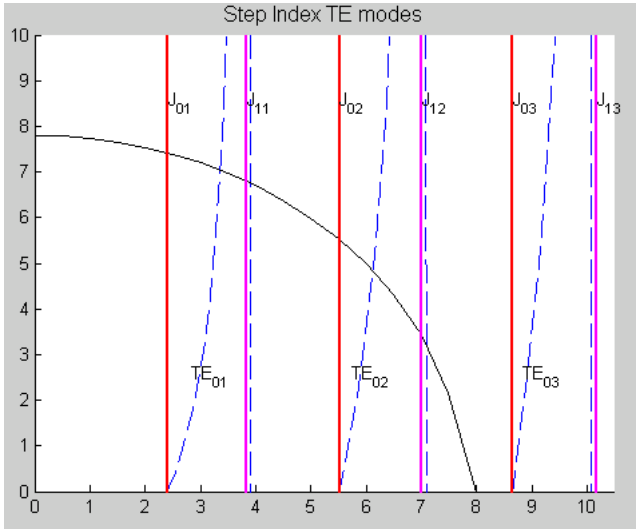

Setting the second term in equation (96) to 0 corresponds to the Transverse Magnetic (TE) Modes

$$\frac{J_1(\kappa a)}{\kappa a J_0(\kappa a)} + \left(\frac{n_2}{n_1}\right)^2 \frac{K_1(\gamma a)}{\gamma a K_0(\gamma a)} = 0 \quad . \tag{96}$$

These modes are named in this manner because setting the above term to 0 causes the coefficient of the longitudinal component of the Magnetic Field to vanish. Therefore, $H_z \to 0$. Hence, only the transverse components of the Magnetic Field remain. Shown in the figure below is a plot of the resulting TM modes, the dashed green lines.

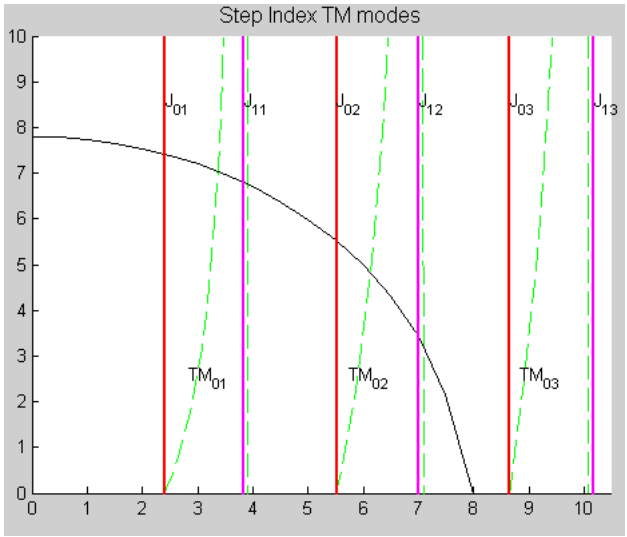

When $\nu \neq 0$, the resulting modes are called skew modes. It is apparent that solving the characteristic equation (89) in this case is much more complicated, and the full derivation will not provided. In the

derivation several approximation must be made to simplify the equation, including the approximations

$$\left(\frac{n_2}{n_1}\right)^2 \approx 1 \quad \text{and} \quad \beta \approx n_1 k \quad . \tag{97}$$

The resulting characteristic equation is

$$\frac{1}{\kappa a}\frac{J'_\nu(\kappa a)}{J_\nu(\kappa a)} + \frac{1}{\gamma a}\frac{K'_\nu(\gamma a)}{K_\nu(\gamma a)} = \pm\nu\left(\frac{1}{(\kappa a)^2} + \frac{1}{(\gamma a)^2}\right) \quad . \tag{98}$$

In the case that the sign in front of the ν is positive, the resulting modes are called HE modes, which have the characteristic equation

$$\frac{J_{\nu-1}(Ka)}{KaJ_\nu(Ka)} - \frac{K_{\nu-1}(\gamma a)}{\gamma a K_\nu(\gamma a)} = 0 \quad . \tag{99}$$

In the case that the sign in front of the ν is negative, the resulting modes are called EH modes, which have the characteristic equation

$$\frac{J_{\nu+1}(Ka)}{KaJ_\nu(Ka)} + \frac{K_{\nu+1}(\gamma a)}{\gamma a K_\nu(\gamma a)} = 0 \quad . \tag{100}$$

8.2 Appendix B: Attempted Solution of 3-layer Fiber BVP

The solution to a multilayer waveguide is at first similar to that for a step-index fiber, which begins by solving Maxwell's equations. The geometry of an optical fiber is cylindrical, so once again the most natural coordinate system to use are the cylidrical coordinates in the proceeding argument, where the coordinates ρ will be use to represent the radial axis, ϕ will be used to represent the azimuthal angle, and z will be used to represent the longitudinal axis. The major difference comes after separating variables to find a function $R(\rho)$, which has the cladding and core terms as before, but also terms for the middle layer.

8.2.1 Discussion

The first step that must be taken is finding the solution to the vectorial wave equations

$$\nabla^2\mathbf{E} + (nk)^2\mathbf{E} = 0 \quad , \tag{1}$$

where $\mathbf{E}$ represents the electric field vector (E_ρ, E_ϕ, E_z), and

$$\nabla^2\mathbf{H} + (nk)^2\mathbf{H} = 0 \quad , \tag{2}$$

where $\mathbf{H}$ represents the electric field vector (H_ρ, H_ϕ, H_z). In both these case, k is the wave number, and n refers to an index number related to the relative permeabilty of a medium by the relation

$$n^2 = \epsilon_r \quad . \tag{3}$$

As different materials have different permeabilities, it is clear that if the optical fiber is made out of layers of different materials then the corresponding index number will be used for each material. As before, the following convention will be used: For a material with N layers, n_i will refer to the index number of the i^{th} layer, for $i = 1, 2...N$, where 1 refers to the inner most, or core, layer. For the step index fiber we had just core (n_1) and cladding (n_2) layers $(N = 2)$. For a three layer fiber we now have the core (n_1), middle (n_2) and cladding (n_3) layers $(N = 3)$.

In cylidrical cooridnates, the Laplacian operator ∇^2 takes the form

$$\nabla^2 = \frac{1}{\rho}\frac{\partial}{\partial\rho}\left(\rho\frac{\partial}{\partial\rho}\right) + \frac{1}{\rho^2}\frac{\partial^2}{\partial\phi^2} + \frac{\partial^2}{\partial z^2} \quad . \tag{4}$$

Thus Eq. (1) becomes

$$\nabla^2\mathbf{E} + (nk)^2\mathbf{E} = \frac{1}{\rho}\frac{\partial}{\partial\rho}\left(\rho\frac{\partial\mathbf{E}}{\partial\rho}\right) + \frac{1}{\rho^2}\frac{\partial^2\mathbf{E}}{\partial\phi^2} + \frac{\partial^2\mathbf{E}}{\partial z^2} + (nk)^2\mathbf{E} = 0 \quad . \tag{5}$$

Similarly, Eq. (2) becomes

$$\nabla^2\mathbf{H} + (nk)^2\mathbf{H} = \frac{1}{\rho}\frac{\partial}{\partial\rho}\left(\rho\frac{\partial\mathbf{H}}{\partial\rho}\right) + \frac{1}{\rho^2}\frac{\partial^2\mathbf{H}}{\partial\phi^2} + \frac{\partial^2\mathbf{H}}{\partial z^2} + (nk)^2\mathbf{H} = 0 \quad . \tag{6}$$

We may proceed by first concidering only the longitudinal component of the electric field.

$$\nabla^2 E_z + (nk)^2 E_z = \frac{1}{\rho}\frac{\partial}{\partial\rho}\left(\rho\frac{\partial E_z}{\partial\rho}\right) + \frac{1}{\rho^2}\frac{\partial^2 E_z}{\partial\phi^2} + \frac{\partial^2 E_z}{\partial z^2} + (nk)^2 E_z = 0 \quad . \tag{7}$$

This equation may be solved by the method of separation of variables, where we assume that E_z is the

product of three independent functions of each coordinate,

$$E_z = R(\rho)\Phi(\phi)Z(z) = R\Phi Z \quad . \tag{8}$$

In this context, Eq. (7) becomes

$$\nabla^2 R\Phi Z + (nk)^2 R\Phi Z = \frac{1}{\rho}\frac{\partial}{\partial\rho}\left(\rho\frac{\partial R\Phi Z}{\partial\rho}\right) + \frac{1}{\rho^2}\frac{\partial^2 R\Phi Z}{\partial\phi^2} + \frac{\partial^2 R\Phi Z}{\partial z^2} + (nk)^2 R\Phi Z \tag{9}$$

$$= R''\Phi Z + \frac{1}{\rho}R'\Phi Z + \frac{1}{\rho^2}R\Phi'' Z + R\Phi Z'' + (nk)^2 R\Phi Z = 0 \quad . \tag{10}$$

Dividing Eq. (10) by $R\Phi Z$ gives

$$\frac{R''}{R} + \frac{R'}{\rho R} + \frac{\Phi''}{\rho^2\Phi} + \frac{Z''}{Z} + (nk)^2 = 0 \quad , \tag{11}$$

or

$$\frac{R''}{R} + \frac{R'}{\rho R} + \frac{\Phi''}{\rho^2\Phi} + (nk)^2 = -\frac{Z''}{Z} = \beta^2 \quad , \tag{12}$$

where β is a yet to be determined. Writing the equation in this manner is possible because the LHS of Eq. (12) is a function of only ρ and ϕ, while $-Z''/Z$ is a function of only z. The only way for these two terms to be equal would be if they were both constant. It follows from $-\frac{Z''}{Z} = \beta^2$ that

$$Z'' + \beta^2 Z = 0 \quad , \tag{13}$$

which has a solution of the form

$$Z(z) = Ae^{j\beta z} + Be^{-j\beta z} \quad , \tag{14}$$

where A & B are yet to be determined constant coefficients, and $j = \sqrt{-1}$. The same method can be used to find $R(\rho)$ and $\Phi(\phi)$ by writing Eq. (12) as

$$\frac{R''}{R} + \frac{R'}{\rho R} + \frac{\Phi''}{\rho^2\Phi} + (nk)^2 - \beta^2 = 0 \quad , \tag{15}$$

and then multiplying by ρ^2 to give

$$\rho^2\frac{R''}{R} + \rho\frac{R'}{R} + \rho^2((nk)^2 - \beta^2) + \frac{\Phi''}{\Phi} = 0 \quad , \tag{16}$$

and recognizing that, in order for this to be true, we must have

$$\rho^2\frac{R''}{R}+\rho\frac{R'}{R}+\rho^2((nk)^2-\beta^2)=-\frac{\Phi''}{\Phi}=\nu^2 \quad . \tag{17}$$

where ν is a yet to be determined. It follows from $-\frac{\Phi''}{\Phi}=\nu^2$ that

$$\Phi''+\nu^2\Phi=0 \quad , \tag{18}$$

which has a solution of the form

$$\Phi(\phi)=Ce^{j\nu\phi}+De^{-j\nu\phi} \quad , \tag{19}$$

where C & D are yet to be determined constant coefficients. The remaining equation is

$$\rho^2\frac{R''}{R}+\rho\frac{R'}{R}+\rho^2((nk)^2-\beta^2)=\nu^2 \quad , \tag{20}$$

which may be rearranged in the form of the Bessel Equation,

$$\rho^2R''+\rho R'+(\rho^2((nk)^2-\beta^2)-\nu^2)R=0 \quad . \tag{21}$$

The functions $Z(z)$ and $\Phi(\phi)$ are the same as those for the step-index fiber. However, for the 3-layer fiber, $R(\rho)$ will be different, due to the term $((nk)^2-\beta^2)$, which is explicitly dependent of the index of the material. Furthermore, this term may be either a positive or negative quanitity. Therefore, as before, let us introduce the terms κ and γ such that

$$(nk)^2-\beta^2=\kappa^2=-\gamma^2 \quad . \tag{22}$$

If we take $((nk)^2-\beta^2)$ to be positive, then Eq. (21) has a solution of the form

$$R(\rho)=EJ_\nu(\kappa\rho)+GN_\nu(\kappa\rho) \quad , \tag{23}$$

where E & G are yet to be determined constant coefficients, and $J_\nu(K\rho)$ & $N_\nu(K\rho)$ are Bessel functions of the first and second kinds, respectively, of order ν. If we take $((nk)^2-\beta^2)$ to be negative, then Eq. (21) has a solution of the form

$$R(\rho)=HI_\nu(\gamma\rho)+FK_\nu(\gamma\rho) \quad , \tag{24}$$

where H & F are yet to be determined constant coefficients, and $I_\nu(\gamma\rho)$ & $K_\nu(\gamma\rho)$ are the modified Bessel functions of the first and second kinds, respectively, of order ν. Inside the core, the term $((nk)^2 - \beta^2)$ is a positive quantity,

$$(n_1 k)^2 - \beta^2 = \kappa^2 \quad , \tag{25}$$

which hints at the use of Eq. (23) with $G = 0$. In the cladding, the term $((nk)^2 - \beta^2)$ is a negative quantity,

$$(n_3 k)^2 - \beta^2 = -\gamma^2 \quad , \tag{26}$$

which hints at the use of Eq. (24) with $H = 0$. Therefore, we may infer a solution of the form

$$R(\rho) = EJ_\nu(\kappa\rho) + FK_\nu(\gamma\rho) + \mathcal{O}(\rho) \tag{27}$$

where the first two terms are from the core and cladding regions, respectively, and the final term is a correction factor to account for the middle layer. For an arbitrary fiber with regions that do not include $\rho = 0$ or $\rho = \infty$, both terms in equations (23) and (24) must be included in the analysis. In the middle layer we have

$$(n_2 k)^2 - \beta^2 = \kappa^2 \quad , \tag{28}$$

near the core boundary, and

$$(n_2 k)^2 - \beta^2 = -\gamma^2 \quad , \tag{29}$$

near the cladding boundary. Therefore the correction term has the form

$$\mathcal{O}(\rho) = L(\rho)J_\nu(\kappa\rho) + M(\rho)N_\nu(\kappa\rho) + P(\rho)I_\nu(\gamma\rho) + Q(\rho)K_\nu(\gamma\rho) \quad , \tag{30}$$

where L, M, P, and Q are coefficients dependent on ρ such that P & $Q \to 0$ as $\rho \to a$, where $\rho = a$ is the boundary between the core and middle layers, and L & $M \to 0$ as $\rho \to b$, where $\rho = b$ is the boundary between the middle layer cladding layers. There terms introduce not only new unknown variables, but also an additional level of complication since the coefficients are not constants. Combining these products gives the general result for the z-component of the Electric field.

$$E_z = \left(EJ_\nu(\kappa\rho)+FK_\nu(\gamma\rho)+L(\rho)J_\nu(\kappa\rho)+M(\rho)N_\nu(\kappa\rho)+P(\rho)I_\nu(\gamma\rho)+Q(\rho)K_\nu(\gamma\rho)\right)\left(Ce^{j\nu\phi}+De^{-j\nu\phi}\right)\left(Ae^{j\beta z}+Be^{-j\beta z}\right) \quad . \tag{31}$$

As before, this result may be simplified by considering only azimuthal rotation in one direction, so

$\Phi(\phi) \rightarrow e^{j\nu\phi}$. Furthermore, since the function Z(z) deals with the longitudinal propagation of the wave, we may limit the consideration to only one direction, $Z(z) \rightarrow e^{j\beta z}$. Finally, by realizing that the constant coefficients are arbitrary and may be included in the $R(\rho)$ coefficients, which would then become new yet to be determined coefficients, and noting that a constant plus an undetermined function of ρ is another undetermined function, we may write

$$E_z = \Big(A(\rho)J_\nu(\kappa\rho) + B(\rho)K_\nu(\gamma\rho) + C(\rho)N_\nu(\kappa\rho) + D(\rho)I_\nu(\gamma\rho) \Big) e^{j\nu\phi} e^{j\beta z} \quad , \tag{32}$$

where A, B, C, and D are the new undetermined coefficient functions. Since the same argument could have been made for the magnetic field, H_z will have a similar form,

$$H_z = \Big(E(\rho)J_\nu(\kappa\rho) + F(\rho)K_\nu(\gamma\rho) + G(\rho)N_\nu(\kappa\rho) + L(\rho)I_\nu(\gamma\rho) \Big) e^{j\nu\phi} e^{j\beta z} \quad , \tag{33}$$

where $E(\rho)$ is analogous to the electric field coefficient $A(\rho)$, $F(\rho)$ to $B(\rho)$, $G(\rho)$ to $C(\rho)$, and $L(\rho)$ to $D(\rho)$.

As before, to find the remaining components of the electric and magnetic fields Maxwell's Equations must be used, or more specifically, Faraday's Law

$$\nabla \times \mathbf{E} = -\mu \frac{\partial \mathbf{H}}{\partial t} \quad , \tag{34}$$

and Ampère's Law

$$\nabla \times \mathbf{H} = \epsilon \frac{\partial \mathbf{E}}{\partial t} \quad . \tag{35}$$

The time dependence of the electric and magnetic fields can be written explicity as

$$\mathbf{E}(\rho, \phi, z, t) = \mathbf{E}(\rho, \phi, z) e^{-j\omega t} \quad , \tag{36}$$

$$\mathbf{H}(\rho, \phi, z, t) = \mathbf{H}(\rho, \phi, z) e^{-j\omega t} \quad , \tag{37}$$

where ω is the corresponding angular velocity, related to the wave number k by the formula

$$(nk)^2 = \omega^2 \mu\epsilon \quad . \tag{38}$$

Therefore, Eqs. (34) & (35) respectively take the forms

$$\nabla \times \mathbf{E} = j\omega\mu\mathbf{H} \quad , \tag{39}$$

$$\nabla \times \mathbf{H} = -j\omega\epsilon\mathbf{E} \quad . \tag{40}$$

Eq. (39) results in the three equations

$$\frac{1}{\rho}\frac{\partial E_z}{\partial \phi} - \frac{\partial E_\phi}{\partial z} = j\omega\mu H_\rho \quad , \tag{41}$$

$$\frac{\partial E_\rho}{\partial z} - \frac{\partial E_z}{\partial \rho} = j\omega\mu H_\phi \quad , \tag{42}$$

$$\frac{1}{\rho}\frac{\partial(\rho E_\phi)}{\partial \rho} - \frac{1}{\rho}\frac{\partial E_\rho}{\partial \phi} = j\omega\mu H_z \quad . \tag{43}$$

Eq. (40) results in the three equations

$$\frac{1}{\rho}\frac{\partial H_z}{\partial \phi} - \frac{\partial H_\phi}{\partial z} = -j\omega\epsilon E_\rho \quad , \tag{44}$$

$$\frac{\partial H_\rho}{\partial z} - \frac{\partial H_z}{\partial \rho} = -j\omega\epsilon E_\phi \quad , \tag{45}$$

$$\frac{1}{\rho}\frac{\partial(\rho H_\phi)}{\partial \rho} - \frac{1}{\rho}\frac{\partial H_\rho}{\partial \phi} = -j\omega\epsilon E_z \quad . \tag{46}$$

For notational simplification in solving these equations, recall the form for E_z,

$$E_z = R(\rho)\Phi(\phi)Z(z) = R\Phi Z \quad , \tag{47}$$

where

$$R(\rho) = R = A(\rho)J_\nu(\kappa\rho) + B(\rho)K_\nu(\gamma\rho) + C(\rho)N_\nu(\kappa\rho) + D(\rho)I_\nu(\gamma\rho) \quad , \tag{48}$$

$$\Phi(\phi) = \Phi = e^{j\nu\phi} \quad , \tag{49}$$

$$Z(z) = Z = e^{j\beta z} \quad . \tag{50}$$

In solving for each component in Maxwell's equations, it will be necessary to take partial derivatives for each of the above terms. The partial of R with respect to ρ is

$$\frac{\partial R(\rho)}{\partial \rho} = M(\rho) = A(\rho)\kappa J'_\nu(\kappa\rho) + B(\rho)\gamma K'_\nu(\gamma\rho) + C(\rho)\kappa N'_\nu(\kappa\rho) + D(\rho)\gamma I'_\nu(\gamma\rho) \quad , \tag{51}$$

where $M(\rho)$ was defined for future convenience. The remaining two partial derivatives are

$$\frac{\partial \Phi(\phi)}{\partial \phi} = j\nu e^{j\nu\phi} = j\nu\Phi \quad , \tag{52}$$

$$\frac{\partial Z(z)}{\partial z} = j\beta e^{j\beta z} = j\beta Z \quad . \tag{53}$$

Eqs. (52) and (53) reveal the apparent simplifications,

$$\frac{\partial}{\partial \phi} = j\nu \quad \text{and} \quad \frac{\partial}{\partial z} = j\beta \quad . \tag{54}$$

Furthermore, let us label the analog of $R(\rho)$ in the magnetic field equation as

$$P(\rho) = P = E(\rho)J_\nu(\kappa\rho) + F(\rho)K_\nu(\gamma\rho) + G(\rho)N_\nu(\kappa\rho) + L(\rho)I_\nu(\gamma\rho) \quad , \tag{55}$$

with partial derivative with respect to ρ

$$\frac{\partial P(\rho)}{\partial \rho} = N(\rho) = E(\rho)\kappa J'_\nu(\kappa\rho) + F(\rho)\gamma K'_\nu(\gamma\rho) + G(\rho)\kappa N'_\nu(\kappa\rho) + L(\rho)\gamma I'_\nu(\gamma\rho) \quad , \tag{56}$$

where $N(\rho)$ was defined for future convenience. We may now write out Eqs. (42) and (44) explicity to solve for E_ρ and H_ϕ. Eq. (42) becomes

$$\frac{\partial E_\rho}{\partial z} - \frac{\partial E_z}{\partial \rho} = j\omega\mu H_\phi \quad . \tag{57}$$

$$j\beta E_\rho - M\Phi Z = j\omega\mu H_\phi \quad . \tag{58}$$

Solving for H_ϕ results in

$$H_\phi = \frac{j\beta E_\rho - M\Phi Z}{j\omega\mu} \quad . \tag{59}$$

Likewise, Eq. (44) becomes

$$\frac{1}{\rho}\frac{\partial H_z}{\partial \phi} - \frac{\partial H_\phi}{\partial z} = -j\omega\epsilon E_\rho \quad . \tag{60}$$

$$\frac{j\nu}{\rho} P\Phi Z - j\beta H_\phi = -j\omega\epsilon E_\rho \quad . \tag{61}$$

Solving for H_ϕ results in

$$H_\phi = \frac{j\omega\epsilon E_\rho + \frac{j\nu}{\rho} P\Phi Z}{j\beta} \quad . \tag{62}$$

Therefore,

$$\frac{j\beta E_\rho - M\Phi Z}{j\omega\mu} = \frac{j\omega\epsilon E_\rho + \frac{j\nu}{\rho}P\Phi Z}{j\beta} \quad , \tag{63}$$

which may be solved for E_ρ to give

$$E_\rho = \frac{(\beta M + \frac{j\omega\mu\nu}{\rho}P)\Phi Z}{j(\beta^2 - \mu\omega^2\epsilon)} \quad . \tag{64}$$

This solution may then be substituted into either Eq. (59) or Eq. (62) to give

$$H_\phi = \frac{(\omega\epsilon M + \frac{j\beta\nu}{\rho}P)\Phi Z}{j(\beta^2 - \mu\omega^2\epsilon)} \quad . \tag{65}$$

Similarly, Eqs. (41) and (45) can be solved to give E_ϕ and H_ρ. The azimuthal component of the electric field is

$$E_\phi = \frac{(\frac{j\beta\nu}{\rho}R - \omega\mu N)\Phi Z}{j(\beta^2 - \mu\omega^2\epsilon)} \quad , \tag{66}$$

and the radial component of the magnetic field is

$$H_\rho = \frac{(-\frac{j\omega\epsilon\nu}{\rho}R + \beta N)\Phi Z}{j(\beta^2 - \mu\omega^2\epsilon)} \quad . \tag{67}$$

It may be noted that the forms of the cylindrical polar components of the Electric and Magnetic Fields are the same as those for a step index fiber. However, the values of R, P, M, and N are different for the 3-layer fiber, and it is with these terms where the difficulties arise.

8.2.2 Attempt at Obtaining the Characteristic Equation

To find the Characteristic Equation of the optical fiber, we begin by applying the boundary condition that the tangential compontents of the electric field (E_z and E_ϕ) and magnetic field (H_z and H_ϕ) must be continuous at the boundary between regions. As noted previously, let $\rho = a$ be the boundary between the core and middle layers, and $\rho = b$ be the boundary between the middle and cladding layers. Recall that

$$R(\rho) = A(\rho)J_\nu(\kappa\rho) + B(\rho)K_\nu(\gamma\rho) + C(\rho)N_\nu(\kappa\rho) + D(\rho)I_\nu(\gamma\rho) \quad , \tag{68}$$

where $A(\rho)$ and $B(\rho)$ both include the sum of a constant term and a coefficient function,

$$A(\rho) = Q + S(\rho) \quad , \tag{69}$$

$$B(\rho) = T + U(\rho) \quad . \tag{70}$$

Likewise

$$P(\rho) = E(\rho)J_\nu(\kappa\rho) + F(\rho)K_\nu(\gamma\rho) + G(\rho)N_\nu(\kappa\rho) + L(\rho)I_\nu(\gamma\rho) \quad , \tag{71}$$

where $E(\rho)$ and $F(\rho)$ both include the sum of a constant term and a coefficient function,

$$E(\rho) = W + X(\rho) \quad , \tag{72}$$

$$F(\rho) = V + Y(\rho) \quad . \tag{73}$$

While new labels were used to distinguish the terms for already defined variables, recall that the coefficient functions S, U, X, & Y arise from the middle layer, the constant terms Q & W arise from the core layer, and T and V arise from the cladding layer. Thus, the z-component of the Electric Field in the core region is

$$E_z(\rho < a) = QJ_\nu(\kappa\rho)e^{j\nu\phi}e^{j\beta z} \quad , \tag{74}$$

in the middle layer is

$$E_z(a < \rho < b) = \Big(S(\rho)J_\nu(\kappa\rho) + U(\rho)K_\nu(\gamma\rho) + C(\rho)N_\nu(\kappa\rho) + D(\rho)I_\nu(\gamma\rho)\Big)e^{j\nu\phi}e^{j\beta z} \quad , \tag{75}$$

and in the cladding region is

$$E_z(\rho > b) = TK_\nu(\gamma\rho)e^{j\nu\phi}e^{j\beta z} \quad . \tag{76}$$

Recall that the coefficient functions were chosen such that U, Y, D & $L \to 0$ as $\rho \to a$, and S, X, C & $G \to 0$ as $\rho \to b$. Therefore, at the boundary $\rho = a$,

$$E_z(\rho = a) = QJ_\nu(\kappa a)e^{j\nu\phi}e^{j\beta z} = \Big(S(a)J_\nu(\kappa a) + C(a)N_\nu(\kappa a)\Big)e^{j\nu\phi}e^{j\beta z} \quad , \tag{77}$$

from which we can solve for one coefficient in terms of the other two to get

$$C(a) = [Q - S(a)]\frac{J_\nu(\kappa a)e^{j\nu\phi}e^{j\beta z}}{N_\nu(\kappa a)e^{j\nu\phi}e^{j\beta z}} = [Q - S(a)]\frac{J_\nu(\kappa a)}{N_\nu(\kappa a)} \quad . \tag{78}$$

At the boundary $\rho = b$,

$$E_z(\rho = b) = TK_\nu(\gamma b)e^{j\nu\phi}e^{j\beta z} = \Big(U(b)K_\nu(\gamma b) + D(b)I_\nu(\gamma b)\Big)e^{j\nu\phi}e^{j\beta z} \quad , \tag{79}$$

from which we can solve for one coefficient in terms of the other two to get

$$D(b) = [T - U(b)]\frac{K_\nu(\gamma b)e^{j\nu\phi}e^{j\beta z}}{I_\nu(\gamma b)e^{j\nu\phi}e^{j\beta z}} = [T - U(b)]\frac{K_\nu(\gamma b)}{I_\nu(\gamma b)} \quad . \tag{80}$$

A similar derivation follows for the z-component of the Magnetic Field to give the results

$$G(a) = [W - X(a)]\frac{J_\nu(\kappa a)}{N_\nu(\kappa a)} \quad , \tag{81}$$

$$L(b) = [V - Y(b)]\frac{K_\nu(\gamma b)}{I_\nu(\gamma b)} \quad . \tag{82}$$

At this point in the calulation for the step-index fiber, there were only two unknown coefficients for the Electric Field terms, which we were able to relate to each other, reducing the number of unknowns to one. The same was true for the Magnetic Field terms, resulting in a total of two unknowns in the problem. This was done using the z-components of the Fields, allowing for the use of the ϕ-component equations of the Fields to write two simultaneous equation, from which the characteristic equation was found. In the case of the 3-layer fiber, for both of the Elecrtic and Magnetic Field terms there are each 6 unknown coefficients, none of which we were able to relate to exactly one other coefficient. While we may be able to use the ϕ-component and ρ-component equations to further reduce the number of unknowns, we would not come to a point where all the unknowns can be cancelled out. Thus, the Boundary Value Problem Approach to solving for a 3-layer fiber breaks down.

8.3 Appendix C: MATLAB code

```
clear;
a = 4*10^(-4);  % inches
b = 16*10^(-4);
c= 99999999999999999;


mu = 4*pi*10^7; %permeability
f=5*10^14;      %Hz
```

```
omega=2*pi*f;  %rad/sec
epsilon_0 = 8.85*10^(-12); %permativity
k_0 = omega/(3*10^8); %wave number
epsilon_r(1) = 2.3;  %core layer
epsilon_r(2) = 2.31; %intermediate layer
epsilon_r(3) = 2.3;  %cladding layer

k(1) = sqrt(epsilon_r(1)*k_0^2);
k(2) = sqrt(epsilon_r(2)*k_0^2);
k(3) = sqrt(epsilon_r(3)*k_0^2);

n(1) = sqrt(epsilon_r(1));
n(2) = sqrt(epsilon_r(2));
n(3) = sqrt(epsilon_r(3));

Beta(1) = k(1)/k_0;  %not used
Beta(2) = k(2)/k_0;  %not used
Beta(3) = k(3)/k_0;  %not used

epsilon_M =  max(epsilon_r);  %max permittivity
epsilon_m =  min(epsilon_r);  %min permittivity

Xi(1) = sqrt(k(1)^2 - Beta(1)^2);  %not used
Xi(2) = sqrt(k(2)^2 - Beta(2)^2);  %not used
Xi(3) = sqrt(k(3)^2 - Beta(3)^2);  %not used

Tau(1) = sqrt(Beta(1)^2 - k(1)^2); %not used
Tau(2) = sqrt(Beta(2)^2 - k(2)^2); %not used
Tau(3) = sqrt(Beta(3)^2 - k(3)^2); %not used

B(1) = sqrt((Beta(1)^2 - epsilon_r(1))/(epsilon_M-epsilon_m)); %not used
```

```
B(2) = sqrt((Beta(2)^2 - epsilon_r(2))/(epsilon_M-epsilon_m)); %not used
B(3) = sqrt((Beta(3)^2 - epsilon_r(3))/(epsilon_M-epsilon_m)); %not used

%M_1 = beta*a*nu*((1./(Xi_1*a).^2)+(1./(Tau(2)*a).^2));
%M_2 = (beta*a*nu/(b/a))*((1/(Tau(3)*a).^2)-(1/(Tau(2)*a).^2));

nu0 = zeros([1  22]);
nu1 = ones([1  22]);
[nuTau20Grid,Tau20]=meshgrid(nu0,linspace(0,30,1000));
[nuTau21Grid,Tau21]=meshgrid(nu1,linspace(0,30,1000));
[nuTau30Grid,Tau30]=meshgrid(nu0,linspace(0,30,1000));
[nuTau31Grid,Tau31]=meshgrid(nu1,linspace(0,30,1000));
[nuXi10Grid,Xi10]=meshgrid(nu0,linspace(0,30,1000));
[nuXi11Grid,Xi11]=meshgrid(nu1,linspace(0,30,1000));

j = sqrt(-1);
% uncomment the following for the explicit imaginary term to be included,
    but you must comment out the similar code directly below
% S_ab = besseli(nuTau20Grid,Tau20*j*a).*besselk(nuTau20Grid,Tau20*j*b)-
    besselk(nuTau20Grid,Tau20*j*a).*besseli(nuTau20Grid,Tau20*j*b);
% S_apb = besseli(nuTau21Grid,Tau21*j*a).*besselk(nuTau20Grid,Tau20*j*b)+
    besselk(nuTau21Grid,Tau21*j*a).*besseli(nuTau20Grid,Tau20*j*b);
% S_abp = -besseli(nuTau20Grid,Tau20*j*a).*besselk(nuTau21Grid,Tau21*j*b)-
    besselk(nuTau20Grid,Tau20*j*a).*besseli(nuTau21Grid,Tau21*j*b);
% S_apbp = -besseli(nuTau21Grid,Tau21*j*a).*besselk(nuTau21Grid,Tau21*j*b)+
    besselk(nuTau21Grid,Tau21*j*a).*besseli(nuTau21Grid,Tau21*j*b);
% R_bc = besseli(nuTau30Grid,Tau30*j*b).*besselk(nuTau30Grid,Tau30*j*c)-
    besselk(nuTau30Grid,Tau30*j*b).*besseli(nuTau30Grid,Tau30*j*c);
% R_bpc = besseli(nuTau31Grid,Tau31*j*b).*besselk(nuTau30Grid,Tau30*j*c)+
    besselk(nuTau31Grid,Tau31*j*b).*besseli(nuTau30Grid,Tau30*j*c);
```

```
% R_bcp = -besseli(nuTau30Grid,Tau30*j*b).*besselk(nuTau31Grid,Tau31*j*c)-
    besselk(nuTau30Grid,Tau30*j*b).*besseli(nuTau31Grid,Tau31*j*c);
% R_bpcp = -besseli(nuTau31Grid,Tau31*j*b).*besselk(nuTau31Grid,Tau31*j*c)+
    besselk(nuTau31Grid,Tau31*j*b).*besseli(nuTau31Grid,Tau31*j*c);

S_ab = besseli(nuTau20Grid,Tau20*a).*besselk(nuTau20Grid,Tau20*b)-besselk(
    nuTau20Grid,Tau20*a).*besseli(nuTau20Grid,Tau20*b);
S_apb = besseli(nuTau21Grid,Tau21*a).*besselk(nuTau20Grid,Tau20*b)+besselk(
    nuTau21Grid,Tau21*a).*besseli(nuTau20Grid,Tau20*b);
S_abp = -besseli(nuTau20Grid,Tau20*a).*besselk(nuTau21Grid,Tau21*b)-besselk
    (nuTau20Grid,Tau20*a).*besseli(nuTau21Grid,Tau21*b);
S_apbp = -besseli(nuTau21Grid,Tau21*a).*besselk(nuTau21Grid,Tau21*b)+
    besselk(nuTau21Grid,Tau21*a).*besseli(nuTau21Grid,Tau21*b);
R_bc = besseli(nuTau30Grid,Tau30*b).*besselk(nuTau30Grid,Tau30*c)-besselk(
    nuTau30Grid,Tau30*b).*besseli(nuTau30Grid,Tau30*c);
R_bpc = besseli(nuTau31Grid,Tau31*b).*besselk(nuTau30Grid,Tau30*c)+besselk(
    nuTau31Grid,Tau31*b).*besseli(nuTau30Grid,Tau30*c);
R_bcp = -besseli(nuTau30Grid,Tau30*b).*besselk(nuTau31Grid,Tau31*c)-besselk
    (nuTau30Grid,Tau30*b).*besseli(nuTau31Grid,Tau31*c);
R_bpcp = -besseli(nuTau31Grid,Tau31*b).*besselk(nuTau31Grid,Tau31*c)+
    besselk(nuTau31Grid,Tau31*b).*besseli(nuTau31Grid,Tau31*c);

%Xi1a
TEmode=(besselj(nuXi11Grid,Xi11*a).*(S_abp+((Tau20*a)./(Tau30*a)).*S_ab))
    ./(besselj(nuXi10Grid,Xi10*a).*((S_apb./(Tau30*a))+(S_apbp./(Tau20*a))))
    ;
TMmode=((epsilon_r(1)*besselj(nuXi11Grid,Xi11*a)).*(S_abp+((epsilon_r(3)*
    Tau20*a)./(epsilon_r(2)*Tau30*a)).*S_ab))./(besselj(nuXi10Grid,Xi10*a)
    .*((S_apb./(Tau30*a))+(epsilon_r(2)*S_apbp./(Tau20*a))));

%Tau2a
```

```
TEmodeTau2=S_apbp./((besselj(nuXi11Grid,Xi11*a)./besselj(nuXi10Grid,Xi10*a)
    ).*(S_abp+(Tau20*a./Tau30*a).*S_ab)-(S_apb./Tau30*a));
TMmodeTau2=epsilon_r(3).*S_apbp./((epsilon_r(1).*besselj(nuXi11Grid,Xi11*a)
    ./besselj(nuXi10Grid,Xi10*a)).*(S_abp+(Tau20*a./Tau30*a).*(epsilon_r(3)/
    epsilon_r(2)).*S_ab)-(S_apb./Tau30*a));

%Tau3
TEmodeTau3 = (S_apb - (besselj(nuXi11Grid,Xi11*a)./((Xi11.*a).*besselj(
    nuXi10Grid,Xi11*a))).*a.*Tau20.*S_ab)./((besselj(nuXi11Grid,Xi11*a)./((
    Xi11.*a).*besselj(nuXi10Grid,Xi11*a))).*S_abp-S_apbp./(a.*Tau20));
TMmodeTau3 = (epsilon_r(3)*S_apb - (besselj(nuXi11Grid,Xi11*a)./((Xi11.*a)
    .*besselj(nuXi10Grid,Xi11*a))).*a.*Tau20*(epsilon_r(3)/epsilon_r(2)).*
    S_ab)./((besselj(nuXi11Grid,Xi11*a)./(Xi11.*a.*besselj(nuXi10Grid,Xi11*a
    ))).*S_abp-S_apbp*epsilon_r(2)./(a.*Tau20));

figure;
plot(a*Tau20, TMmode,'.')
hold on;
xlim([0 10.5])
ylim([0 10])
title('\xi_1*a Characteristic TM curves','FontSize',12);
ylabel('\xi_1*a');
xlabel('\tau_{2}*a');

figure;
plot(a*Tau20, TEmode,'.')
hold on;
xlim([0 10.5])
ylim([0 10])
title('\xi_1*a Characteristic TE curves','FontSize',12);
ylabel('\xi_1*a');
```

```
xlabel('\tau_{3}*a');

figure;
plot(a*Tau30, TMmodeTau2,'.')
hold on;
xlim([0 10.5])
ylim([0 10])
title('\tau_{2}*a Characteristic TM curves','FontSize',12);
ylabel('\tau_{2}*a');
xlabel('\xi_1*a');

figure;
plot(a*Tau30, TEmodeTau2,'.')
hold on;
xlim([0 10.5])
ylim([0 10])
title('\tau_{2}*a Characteristic TE curves','FontSize',12);
ylabel('\tau_{2}*a');
xlabel('\xi_1*a');

% figure;
% plot(a*Xi10, TMmodeTau3,'.')
% hold on;
% xlim([0 10.5])
% ylim([0 10])
% title('Three Layer Fiber Tau3*a TM modes','FontSize',12);
% ylabel('Tau3*a');
%
% figure;
% plot(a*Xi10, TEmodeTau3,'.')
% hold on;
```

```
% xlim([0  10.5])
% ylim([0  10])
% title('Three Layer Fiber Tau3*a TE modes','FontSize',12);
% ylabel('Tau3*a');


TEdataX = zeros(1000,1000);
TEdataY = zeros(1000,1000);
TEiMax = length(TEmode);
TEDivSize = 100;
TEerr = .1;
for R=1:1000
    Vp = R/TEDivSize;
    for i=1:TEiMax
        if((abs(TEmode(i))>0)&&((Vp^2 - TEerr) < (TEmode(i)^2 + (a*Tau20(i))
            ^2))&& ((TEmode(i)^2 + (a*Tau20(i))^2) < (Vp^2 + TEerr)))
            TEdataY(R,i) = TEmode(i);
            TEdataX(R,i) = Tau20(i);
        end
    end
end
[TErows,TEcols,TEvals] = find(TEdataY);
figure;
plot(TErows/TEDivSize,TEvals,'.');
xlabel('V = sqrt((k_0*a)^2*(\epsilon_1 - \epsilon_3))');
ylabel('Xi1')
title('Xi1 TE modes');
xlim([0  10.5])
ylim([0  10])

TMdataX = zeros(1000,1000);
```

```
TMdataY = zeros(1000,1000);
TMiMax = length(TMmode);
TMDivSize = 100;
TMerr = .1;
for R=1:1000
    Vp = R/TMDivSize;
    for i=1:TMiMax
        if((abs(TMmode(i))>0)&&((Vp^2 - TMerr) < (TMmode(i)^2 + (a*Tau20(i))
            ^2))&& ((TMmode(i)^2 + (a*Tau20(i))^2) < (Vp^2 + TMerr)))
            TMdataY(R,i) = TMmode(i);
            TMdataX(R,i) = Tau20(i);
        end
    end
end
[TMrows,TMcols,TMvals] = find(TMdataY);
figure;
plot(TMrows/TMDivSize,TMvals,'.');
xlabel('V = sqrt((k_0*a)^2*(\epsilon_1 - \epsilon_3))')
title('\xi_1 TM modes');
ylabel('\xi_1')
xlim([0  10.5])
ylim([0  10])

TE2dataX = zeros(1000,1000);
TE2dataY = zeros(1000,1000);
TE2iMax = length(TEmodeTau2);
TE2DivSize = 100;
TE2err = .1;
for R=1:1000
    Vp = R/TE2DivSize;
    for i=1:TE2iMax
```

```
        if((abs(TEmodeTau2(i))>0)&&((Vp^2 - TE2err) < (TEmodeTau2(i)^2 + (a*
            Tau20(i))^2))&& ((TEmodeTau2(i)^2 + (a*Tau20(i))^2) < (Vp^2 +
            TE2err)))
             TE2dataY(R,i) = TEmodeTau2(i);
             TE2dataX(R,i) = Tau20(i);
        end
    end
end
[TE2rows,TE2cols,TE2vals] = find(TE2dataY);
figure;
plot(TE2rows/TE2DivSize,TE2vals,'.');
xlabel('V = sqrt((k_0*a)^2*(\epsilon_1 - \epsilon_2))');
title('\tau_{2} TE modes');
ylabel('\tau_{2}')
xlim([0 10.5])
ylim([0 10])

TM2dataX = zeros(1000,1000);
TM2dataY = zeros(1000,1000);
TM2iMax = length(TMmodeTau2);
TM2DivSize = 100;
TM2err = .1;
for R=1:1000
    Vp = R/TM2DivSize;
    for i=1:TM2iMax
        if((abs(TMmodeTau2(i))>0)&&((Vp^2 - TM2err) < (TMmodeTau2(i)^2 + (a*
            Tau20(i))^2))&& ((TMmodeTau2(i)^2 + (a*Tau20(i))^2) < (Vp^2 +
            TM2err)))
             TM2dataY(R,i) = TMmodeTau2(i);
             TM2dataX(R,i) = Tau20(i);
        end
```

```
    end
end
[TM2rows,TM2cols,TM2vals] = find(TM2dataY);
figure;
plot(TM2rows/TM2DivSize,TM2vals,'.');
xlabel('V = sqrt((k_0*a)^2*(\epsilon_1 - \epsilon_2))')
ylabel('\tau_{2}')
title('\tau_{2} TM modes');
xlim([0  10.5])
ylim([0  10])
```